A Novel Approach Based on Modified and Hybrid Flower Pollination Algorithm to Solve Multi-objective Optimal Power Flow

Gonggui Chen, Qilin Qin, Zhou Ping, Kang Peng, Xianjun Zeng, Hongyu Long* and Mi Zou

Abstract—**In this paper, a modified and hybrid flower pollination algorithms (MHFPA) is proposed for dealing with the multi-objective optimal power flow (MOOPF) problem with conflictive objectives. The algorithm combines the mutation and crossover process in the differential evolution (DE) algorithm, introduces the sinusoidal nonlinear dynamic switching probability (SNDSP) and the elite strategy of elder generation (ESEG), which can improve the shortcomings of the original pollen algorithm that it is easy to fall into the local optimum and the diversity is insufficient. A screening approach with Pareto-dominant rule (SAPR) is proposed to ensure that the state variable can satisfy the inequality constraints of the power system. A uniformly distributed Pareto optimal set (POS) is obtained by the non-dominant sorting with elite strategy (NSES) based on Rank and Density estimation, and the best trade-off solution (BTS) is determined from the POS obtained by the fuzzy affiliation theory. For practicality, the total fuel cost, active power loss, emissions and voltage deviation are selected as objective functions. Due to the limitations of the actual power system, the valve point effect is also considered. The IEEE30-, 57- and IEEE118-bus test systems are used to verify the performance of the proposed MHFPA. In addition, two performance indicators, Hypervolume (HV) and Spacing (SP), quantitatively evaluate the diversity and uniformity of the POS obtained by MHFPA. The simulation results show that, compared with the classic MOPSO and NSGA-II algorithms, the method proposed in this paper shows a greater competitive advantage in dealing with different scales and non-convex optimization problems.**

Index Terms—**Modified and hybrid FPA, Pareto optimal set, optimal power flow, non-dominant sorting, performance indicators**

Manuscript received June 7, 2021; revised October 15, 2021. This work was supported by the National Natural Science Foundation of China (51207064), the Chongqing Natural Science Foundation (cstc2020jcyj-msxmX0368), the Science and Technology Research Program of Chongqing Municipal Education Commission (KJQN201900627), the Natural Science Foundation of Chongqing(cstc2020jcyj-msxmX0693), the National Natural Science Foundation of China(52007022),and the China Postdoctoral Science Foundation(2021M693930).

Gonggui Chen is a professor of Key Laboratory of Industrial Internet of Things and Networked Control, Ministry of Education, Chongqing University of Posts and Telecommunications, Chongqing 400065, China; Chongqing Key Laboratory of Complex Systems and Bionic Control, Chongqing University of Posts and Telecommunications, Chongqing 400065, China (e-mail: chenggpower@ 126.com).

Qilin Qin is a master degree candidate of Chongqing University of Posts and Telecommunications, Chongqing 400065, China (e-mail: 15084418828@163.com).

Ping Zhou is a senior engineer of Economic and Technology Research Institute, State Grid Chongqing Electric Power Company, Chongqing 401120, China(e-mail: 153326062@qq.com) .

Peng Kang is a senior engineer of Economic and Technology Research Institute, State Grid Chongqing Electric Power Company, Chongqing 401120, China(e-mail: 1060846892@qq.com) .

Xianjun Zeng is a senior engineer of State Grid Chongqing Electric Power Company, Chongqing 400015, China (e-mail: 13594255525@139.com).

Hongyu Long is a professor level senior engineer of Chongqing Key Laboratory of Complex Systems and Bionic Control, Chongqing University of Posts and Telecommunications, Chongqing 400065, China(corresponding author to provide phone: +8613996108500; e-mail: longhongyu20@163.com).

Mi Zou is an assistant professor of Chongqing Key Laboratory of Complex Systems and Bionic Control, Chongqing University of Posts and Telecommunications, Chongqing 400065, China(e-mail: zoumi@cqupt.edu.cn).

I. INTRODUCTION

THE Optimal Power Flow (OPF) proposed by Carpentier in 1962 is one of the challenges of the economic operation of the power system, which has attracted wide attention from many experts and scholars [1]. The optimal power flow problem is one of the basic problems of a given or fixed load power. It involves the dispatching of the actual power of all generators, the generator bus voltage, the tap ratio of the transformer and the setting of VAR, and it is subject to the physical properties and electrical constraints of the system. At the same time, it is also a non-linear problem, trying to minimize the fuel cost or active power loss by adjusting the value of the control variable, while satisfying the equality and inequality constraints in the power system [2, 3]. However, with the continuous growth of power demand and people's more and more concerns about the environment, the traditional single-objective optimal power flow model can not meet the demand. To simulate OPF model more realistically, the voltage deviation and emission must be taken as part of the objective function of OPF. Therefore, this paper takes a novel methods to address the multi-objective problems in the power system [4-8].

Multi-objective optimization power flow is a large-scale, highly nonlinear and non-convex optimization problem [9]. Different from the single objective optimization problem, the solution of the multi-objective optimization problem is composed of a set of solutions rather than only one solution. It's very difficult to solve this problem, because it requires very clever technology [10]. In the past, in order to solve large-scale non-convex nonlinear constrained optimization problems, different parameters were set for objective functions on the basis of the priority of objective functions, which was transformed into an optimization problem with only one objective function by weighted sum [11]. However, the weight coefficients are artificially decided, which will have a great impact on the final result. In addition, it is almost impossible to find a well-distributed POS with a traditional method in the face of high-dimensional and complex systems.

In recent years, with the rapid development of computer technology, some classical heuristic algorithms have come to the fore [12-15]. Many researchers have tried to solve the MOOPF problem with heuristic algorithms, such as: improved bat algorithm [16], hybrid self-adaptive FAHSPSO DE algorithm [17], quasi-oppositional modified Jaya algorithm [18], multi-object beetle antennae search algorithm with BAS-BP fuel cost forecast network [19], dynamic population artificial bee colony algorithm [20], improved moth-flame optimization algorithm [21], modified pigeon-inspired optimization algorithm [22], dimension based firefly algorithm [23], hybrid Firefly-Bat Algorithm [24]. The results show that the heuristic algorithms are very feasible methods to solve the MOOPF problem.

Flower pollination algorithm (FPA) was put forward to solve the MOOPF problem by Xin-She Yang in 2014 [25]. Due to the simple structure and few parameters of FPA, the algorithm is widely used in various fields [26]. However, the original FPA algorithm still has the disadvantages of slow convergence speed, easy to fall into local optimality and insufficient diversity [27]. In response of the above weaknesses, this paper proposes a modified and hybrid flower pollination algorithm based on the mutation and crossover process of DE algorithm, SNDSP and ESEG to deal with the MOOPF problem. As far as we know, this improved method is the first time used to solve the MOOPF problem. In order to verify the performance and practicability of the proposed algorithm, MHFPA is tested on three different dimensional test systems of IEEE30, IEEE57 and IEEE118, and the results obtained are compared with the recently published literatures. The results show that the proposed method has better performance.

The rest of this paper is organized as follows: The mathematical formulation of MOOPF problem and three multi-objective optimization strategies are presented in Section II. Section III introduces the application of MHFPA algorithm in MOOPF. Simulating studies on three different-scale systems and the performance analysis are given in Section IV. Finally, Section V concludes this work.

II. Formulation of MOOPF Problem

The MOOPF problem generally considers two or more objectives, including voltage deviation, fuel cost, active power loss, emission and fuel cost with valve-point, etc. On the premise of satisfying the equality constraints and inequality constraints, the objective functions needed by decision-makers are optimized simultaneously [28-30]. The mathematical model of MOOPF is as follows:

$$Min \quad J(x,u)=\left\{J_1(x,u),\cdots J_i(x,u),\cdots J_m(x,u)\right\} \tag{1}$$

$$G_i(x,u)=0, \quad i=1,2,\cdots GL \tag{2}$$

$$H_j(x,u)\le 0, \quad j=1,2,\cdots HL \tag{3}$$

where J_1, J_2, and J_m are the objective functions to be optimized. m is the count of objectives. $G_i(x,u)$ and $H_j(x,u)$ represent the ith equality constraint and the jth inequality constrain, respectively. GL is the number of equality limits, and HL is the count of inequality limits.

x^{T} represents the vector of state variables, including active power output of the slack bus, P_{Gslack} load bus voltage magnitude V_L, reactive output power of generators Q_{Ge}, transmission line loading S_{TL}. It can be defined as:

$$x^{\mathrm{T}}=\left[P_{Gslack},V_{L_1}\ldots V_{L_{NPQ}},Q_{Ge_1}\ldots Q_{Ge_{NG}},S_{TL_1}\ldots S_{TL_{NTL}}\right] \tag{4}$$

u^{T} is the vector of control variables including the output active power of generators except the slack bus P_{Ge}, the voltage magnitude of generators V_{Ge}, the injected reactive power of shunt compensators Q_{Co}, the tap setting of the transformers T, It can be written as:

$$u^{\mathrm{T}}=\left[P_{Ge_2},..,P_{Ge_{NG}},V_{Ge_1},..,V_{Ge_{NG}},Q_{Co_1},..,Q_{Co_{NC}},..,T_1,..T_{NT}\right] \tag{5}$$

where NPQ is the number of load buses. NTL is the number of transmission lines. NG is the count of generators. NC is the count of shunt compensators, and NT is the count of regulating transformers.

A. Objective Functions

In this paper, basic fuel cost, fuel cost with value-point loading, emission, active power loss and voltage magnitude deviation are considered to demonstrate the performance of the proposed method.

1) Basic Fuel Cost Minimization

This is the most commonly used mathematical model to calculate the total fuel cost in OPF problems. It is expressed as:

$$J_{fcost}=\sum_{i=1}^{NG}(a_i+b_iP_{Gei}+c_iP_{Gei}{}^2)\ \$/\mathrm{h} \tag{6}$$

where J_{fcost} is basic fuel cost. a_i, b_i and c_i are the cost coefficients of the ith generator, and P_{Gei} is the active power of the ith generator.

2) Fuel Cost with Valve-point Loadings Minimization

Due to the consideration of the valve point effect, this objective function is significantly different from (6). In other words, the model is more realistic.

$$J_{cost\text{-}vp}=\sum_{i=1}^{NG}[a_i+b_iP_{Gei}+c_iP_{Gei}^2+\left|d_i\sin(e_i(P_{Gei}^{\min}-P_{Gei}))\right|]\ \$/\mathrm{h} \tag{7}$$

where $J_{cost\text{-}vp}$ is the fuel cost with value-point loadings of the tested system. d_i and e_i represent cost coefficients of the ith generator.

3) Emission Objective Minimization

The emission of SOx and NOx from thermal power plants is the main cause of environmental pollution. In this paper, the exhaust emission model is established based on the appropriate weighted summation of these two types of emission gases. The objective function can be stated as follows:

$$J_{emission}=\sum_{i=1}^{NG}[\alpha_iP_{Gei}^2+\beta_iP_{Gei}+\gamma_i+\zeta_i\exp(\lambda_iP_{Gei})]\ \mathrm{ton/h} \tag{8}$$

where α_i, β_i, γ_i, ζ_i and λ_i are the emission coefficients of ith generator.

4) Active Power Loss Minimization

Transmission loss is inevitable in the process of power transmission. Reducing actual transmission loss is one of the important goals of the OPF problem.

$$J_{Ploss}=\sum_{k=1}^{NTL}G_{k(i,j)}[V_i^2+V_j^2-2V_iV_j\cos(\delta_i-\delta_j)]\ \mathrm{MW} \tag{9}$$

where J_{ploss} is the total active power losses of the power system. G_k is the conductance of the kth line. δ_i and δ_j are the voltage angle of node i and j, respectively. Vi and V_j are the voltage magnitude of node i and j, respectively.

5) Voltage Magnitude Deviation Minimization

Voltage deviation is an important quality and safety index, and its magnitude has a direct influence on the stability and economic benefit of the power system. It can be described as below:

$$J_{VD} = \sum_{i=1}^{NPQ} |V_i - 1.0| \tag{10}$$

where J_{VD} represents the total voltage deviation of the tested system.

B. Problem Constrains

It makes sense to optimize the five objective functions only when both equality and inequality constraints of the power system are satisfied.

1) Equality Constrains

Equality constraints include active and reactive power balance [31, 32], which can be depicted as:

$$P_{Gi} - P_{Di} = V_i \sum_{j=1}^{Nb} V_j (G_{ij} \cos(\delta_i - \delta_j) - B_{ij} \sin(\delta_i - \delta_j)) \quad \forall i \in Nb \tag{11}$$

$$Q_{Gi} - Q_{Di} = V_i \sum_{j=1}^{Nb} V_j (G_{ij} \sin(\delta_i - \delta_j) + B_{ij} \cos(\delta_i - \delta_j)) \quad \forall i \in Nb \tag{12}$$

where P_{Gi} and Q_{Gi} are the value of active and reactive power of ith generator. P_{Di} and Q_{Di} stand for the demand of active and reactive power at load bus i. G_{ij} and B_{ij} represent the conductance and susceptance between node i and j, respectively. Nb denotes the count of all buses of the power system.

2) Inequality Constrains

Inequality constraints are composed of state variable constraints and control variable constraints to limit the system variables within the effective range [33].

(1) Inequality constrains of control variables

(i) Active power P_G constrains

$$\begin{matrix} P_{Gei}^{\max} - P_{Gei} \ge 0 \\ P_{Gei} - P_{Gei}^{\min} \ge 0 \end{matrix}, \ i \in NG(i \ne slack) \tag{13}$$

(ii) Voltage V_G constrains

$$\begin{matrix} V_{Gei}^{\max} - V_{Gei} \ge 0 \\ V_{Gei} - V_{Gei}^{\min} \ge 0 \end{matrix}, \ i \in NG \tag{14}$$

(iii) Transformer tap-settings T constrains

$$\begin{matrix} T_i^{\max} - T_i \ge 0 \\ T_i - T_i^{\min} \ge 0 \end{matrix}, \ i \in NT \tag{15}$$

(iv) Reactive power sources Q_C constrains

$$\begin{matrix} Q_{Coi}^{\max} - Q_{Coi} \ge 0 \\ Q_{Coi} - Q_{Coi}^{\min} \ge 0 \end{matrix}, \ i \in NC \tag{16}$$

(2) Inequality constrains of state variables

(i) Active power at slack bus P_{Gslack} constrains

$$P_{Gslack}{}^{\max} \le P_{Gslack} \le P_{Gslack}{}^{\min} \tag{17}$$

(ii) Voltages at load buses VL constrains

$$\begin{matrix} V_{Li}^{\max} - V_{Li} \ge 0 \\ V_{Li} - V_{Li}^{\min} \ge 0 \end{matrix}, \ i \in NPQ \tag{18}$$

(iii) Apparent power S constrains

$$S_{ij}^{\max} \ge S_{ij}, \ ij \in NTL \tag{19}$$

(iv) Reactive power Q_G constrains

$$\begin{matrix} Q_{Gei}^{\max} - Q_{Gei} \ge 0 \\ Q_{Gei} - Q_{Gei}^{\min} \ge 0 \end{matrix}, \ i \in NG \tag{20}$$

C. Multi-objective Problem Solving Strategies

In the actual MOOPF problem, the objectives are often interacting, competing, and coupled together. In addition, their solutions are a set of solutions, and the decision maker cannot make a choice on the optimal solution. In order to obtain POS with high quality and uniform distribution and the BTS, three strategies are proposed to solve the above problems.

1) Constraint Handling Strategies

The Newton-Raphson flow calculation can verify whether each solution violates the equality constraints (11) and (12). Control variable and state variable constraints are called inequality constraints. Once the constraints are violated, the solution is invalid. For the control variable constraints, once any individual control variable exceeds its own constraint range, it is updated and adjusted in the following way:

$$u_i = \begin{cases} u_i & if \ u_{i,\min} < u_i < u_{i,\max} \\ u_{i,\min} & if \ u_i < u_{i,\min} \\ u_{i,\max} & if \ u_i > u_{i,\max} \end{cases} \tag{21}$$

For the inequality constraint processing of state variables, SAPR is proposed to solve this problem, and it is obviously different from the traditional penalty coefficient method. Its core steps are as follows:

Step1: Calculate the violation of inequality constrains for ith individual $total\_vio(u_i)$ based on(22).

$$total\_vio(u_i) = \sum_{j=1}^{HL} \max(\mathrm{G}_j(x, u_i), 0) \tag{22}$$

where HL is the count of inequality constrains on state variables.

Step2: Two different control variables u_1 and u_2 are randomly selected, and their total constraint violation $total\_vio(u_1)$ and $total\_vio(u_2)$ are compared.

Step3: Judge the dominant relationships of the vectors u_1 and u_2. The key theory can be described as below:

$$\begin{cases} \forall i \in (1,2,\dots,m), & J_i(x,u_2) \le J_i(x,u_1) \\ \exists j \in (1,2,\dots,m), & J_j(x,u_2) < J_j(x,u_1) \end{cases} \tag{23}$$

Step4: if u_2 dominates u_1, u_2 is regarded as the Pareto optimum solution.

2) Non-dominant Sorting with Elite Strategy

In 2002, Deb proposed a non-dominated sorting with elite strategy, and obtained a uniformly distributed Pareto front [14]. In this approach, Deb put forward two important concepts: Rank and Density Estimation.

(1) Rank

Let's assume that each pollen individual i has two parameters $o(i)$ and $m(i)$. $o(i)$ is the quantity of individuals that dominate individual i. $m(i)$ is the quantity of individuals dominated by individual i. The rules to determine the Rank are defined as below:

(i) Find all individuals with $o(i)$=0 in the population, and put them into the set G and marked as $Rank$=1;

(ii) For each individual j in the current G, we investigate the number of individual $m(j)$ it dominate, and subtract 1 from $o(k)$ of each individual k in the set $m(j)$. If $o(k)$-1=0, then individual k is put into another set E and marked as *Rank*=2;

(iii) Repeat steps (i) and (ii) until all pollen have their own *Rank*.

(2) Density Estimation

By calculating the average distance of each objective of the two adjacent points of a certain solution in the population, the density estimate $D_{estimation}$ of the point can be obtained, which is also called the crowding distance. After determining the ranks of the solution set, some ranks may contain multiple optimal Pareto solutions, in which case, the density estimate $D_{estimation}$ can be used as the basis for screening. Usually, there are multiple optimal Pareto solutions at the same rank, and the individuals with larger density estimates are preferred. $D_{estimation}$ can be calculated according to formula (24).

$$D_{estimation}(i)=\sum_{j=1}^{H}\frac{J_j(i+1)-J_j(i-1)}{J_{j,\max}-J_{j,\min}} \tag{24}$$

where H is the number of objective functions. $J_j(i)$ represents the value of the jth objective function of the ith solution. $J_{i,\max}$ and $J_{j,\min}$ are the maximum and minimum values of the jth objective function in the Pareto front solution set, respectively.

(3) Best Trade-off Solution

The Pareto front solution set can be considered as optimal results, and there are no superior or inferior relations. In actual engineering practice, according to the current needs of decision makers, the most suitable solution is determined from the POS set, which is called the best trade-off solution (BTS). In this paper, the fuzzy theory based on satisfaction is used to determine the BTS of MOOPF problem. The satisfaction function $M_{i,j}$ and the satisfaction value $Sat(j)$ of the jth pollen on the ith objective can be calculated by formulas (25) and (26).

$$M_{i,j}=\begin{cases} 1 & J_i < J_{i,\min} \\ \dfrac{J_{i,\max}-J_i}{J_{i,\max}-J_{i,\min}} & J_{i,\min} < J_i < J_{i,\max} \\ 0 & J_i < J_{i,\max} \end{cases} \tag{25}$$

$$i=1,2,\ldots,H \quad j=1,2,\ldots N$$

$$Sat(j)=\frac{\sum_{i=1}^{H}M_i^j}{\sum_{j=1}^{N}\sum_{i=1}^{H}M_i^j} \tag{26}$$

where N is the size of the POS set. $J_{i,\max}$ and $J_{i,\min}$ are the maximum and minimum values of the ith objective, respectively. The solution with the largest satisfaction value $Sat(j)$ in the POS set is the BTS solution determined by the fuzzy affiliation theory.

III. Proposed Hybrid Approach

The basic flower pollination algorithm has advantages such as simplicity and flexibility. In terms of parameters, the FPA has only a few parameters, including the switching probability P and scaling factor γ and ζ. It has been used to solve economic scheduling problems [34] and wind speed prediction problems [35]. However, the FPA still has the shortcomings of slow convergence speed, easy to fall into local optimum and insufficient diversity. To address these deficiencies, the improved and hybrid flower pollination algorithm is proposed.

A. Overview of Standard Flower Pollination Algorithm

Inspired by the pollination process of flowering plants in nature, Yang first proposed a new intelligence optimization algorithm FPA in 2012. In the normative FPA, the pollen represents the optimal solution. To mimic pollination, FPA follows four rules, and the details are shown in literature [36].

The pollination process of FPA is divided into local and global pollination. If the switching probability P is greater than the random number *rand*, the algorithm performs global pollination. The global pollination process can be described by formula (27):

$$F_i(t+1)=F_i(t)+\gamma L(\lambda)(F_{elite}(t)-F_i(t)) \tag{27}$$

where $F_i(t)$ is the pollen i at iteration t. $F_{elite}(t)$ is the best solution among all solutions of the current generation. γ is a scaling factor to control the step size.

The introduction of parameter $L(\lambda)$ can better simulate the trajectory of pollinators. $L(\lambda)$ is the Lévy-flights based step size, that corresponds to the pollination power. It obeys a Lévy distribution:

$$L\sim\frac{\lambda\Gamma(\lambda)\sin(\pi\lambda/2)}{\pi}\frac{1}{s^{1+\lambda}},\quad (s>>s_0>0) \tag{28}$$

where $\Gamma(\lambda)$ is called the standard gamma function and the distribution factor λ is set to 1.5 in basic FPA [36].

During local pollination, each flower updates its own position based on the differences between its current position and the positions of two neighboring flowers. It can also be expressed according to Eq (29):

$$F_i(t+1)=F_i(t)+\zeta(F_m(t)-F_n(t)) \tag{29}$$

where $F_m(t)$ and $F_n(t)$ represent pollen from different flowers of the same plant species. ζ represents a random number controlling local walk, which is selected from a uniform distribution [0, 1]. The switching probability P is a key parameter, which coordinates the global search and local search of the algorithm. In reference [37], the value of P is set to 0.8. Preliminary research shows that P=0.8 may be better for most problems.

B. Proposed MHFPA

Three strategies of SNDSP, ESEG and SAPR are proposed to modify the FPA algorithm

1) Sinusoidal nonlinear dynamic switching probability

In the normative FPA, Yang believes that P=0.8 has the best optimization effect after many tests. However, Salgotra studies show that dynamic switching probability is more conducive to coordinating global and local optimization. In this paper, the SNDSP is proposed. It can be described as below:

$$P=(P_{\max}-P_{\min})\sin(\frac{\pi}{2}\frac{t}{T_{\max}})+P_{\min} \tag{30}$$

where $T_{\max}$ corresponds to the maximum number of iterations. t is the number of current iterations. $P_{\min}$ and $P_{\max}$ are set as 0.2 and 0.8, respectively. Compared with P in literature [38], the switching probability P in this paper has a wider variation range, which makes the algorithm have different optimization focuses on different iteration stages.

2) Elite Strategy of Elder Generation

The local optimization process is highly random. In the face of high-dimensional, non-convex nonlinear MOOPF problem, the basic FPA is easy to fall into the local optimal, resulting in inaccurate results. In view of these defects, elite pollen is introduced to increase the ability of pollen to search for the best and to jump out of the local optimal. The above process can be expressed by formula (31):

$$F_i(t+1) = F_i(t) + \zeta(F_m(t) - F_n(t)) + G_{corr} \tag{31}$$

$$G_{corr} = rand(\sigma_1|F_{elite}(t) - F_i(t)| + \sigma_2|F_{elite}(t-1) - F_i(t)|) \tag{32}$$

$$\begin{aligned} \sigma_1 &= \sigma_{\min} + (t/T_{\max})(\sigma_{\max} - \sigma_{\min}) \\ \sigma_2 &= \sigma_{\max} - (t/T_{\max})(\sigma_{\max} - \sigma_{\min}) \end{aligned} \tag{33}$$

where $F_{elite}(t)$ and $F_{elite}(t\text{-}1)$ are the best pollens at tth and (t-1)th iteration, respectively. σ_1 and σ_2 are the scale factors. G_{corr} represents the correction factor.

3) Mutation and Crossover Operator of DE Algorithm

The mutation and crossover process of DE algorithm are introduced into global search to improve the insufficient of diversity in the original FPA [39].

Its updated formula of the mutation process of DE algorithm is as follows:

$$M\_F_i(t+1) = F_{l1}(t) + \psi(F_{l2}(t) - F_{l3}(t)) \tag{34}$$

where $l1$, $l2$ and $l3$ are random numbers different from i. $M\_F_i(t+1)$ represents the mutated individual i. Ψ is a real constant, which controls the process of mutation. $F_{l1}(t)$, $F_{l2}(t)$ and $F_{l3}(t)$ represent random individuals different from individual i, respectively.

The corresponding updated formula of the crossover process is as follows:

$$F_{i,d}(t+1) = \begin{cases} M\_F_{i,d}(t+1), & if\ rand(0,1) \le cr \,\|\, d = d_{rand} \\ F_{i,d}(t), & otherwise \end{cases} \\ d = 1, 2, \ldots, D \tag{35}$$

where D and d represent the dimension of the control variable and the dth control variable, respectively. cr is the crossover constant, which represents the possibility of crossover. d_{rand} is a random number in {1,2,…,D}.

It is worth noting that mutation is not an inevitable process in nature. In this paper, we set the probability of mutation P_m as 0.5, which not only keeps the original pollen individuals, but also increases the diversity of pollen and improves the global search ability.

The pseudo-code of MHFPA is presented in TABLE I.

IV. Simulation Results And Discussion

In order to verify the effectiveness of MHFPA, the performance of the proposed algorithm is tested on three power systems with different scales: IEEE30, IEEE57 and IEEE118, and ten different cases are listed TABLE II. The process of dealing with the MOOPF problem with the proposed method is shown in Fig. 1. Source code of three optimized algorithms are implemented in MATLAB R2018b software in a PC with Intel(R) Core(TM) i5-7400CPU @ 3.00GHz with 8GB RAM.

A. Test Systems

Fig. 2 shows the structure of the IEEE30 standard test system. The system has 6 generators, 30 buses, 4 transformers, 9 reactive power compensation devices and a set of 24-dimensional control variables. Detailed data such as fuel cost coefficient and emission coefficient can be found in the literature [24, 40]. The voltage variation range of generator and load bus are both 0.95 to 1.1 p.u, and the lower limit of the transformer tap is 0.9 p.u and the upper limit is 1.1 p.u.

Fig. 3 shows the structure of the IEEE57 standard test system, and its detailed data refers to literature [23, 24]. The system contains a set of 33-dimensional control variables, 7 generators and 17 transformers. The upper and lower limits of the transformer tap, the voltage of PQ and PV node are 1.1 p.u and 0.9 p.u, respectively. Finally, the variation range of the shunt capacitors is controlled between 0 and 0.3 p.u.

TABLE I
PSEUDO-CODE OF MHFPA METHOD

```
Input: objective function: J(x,u)={J1(x,u),…, Ji(x,u),…, Jm(x,u)};
The pollen population is randomly initialized within the constraint range;Set MHFPA parameters: switch probability P, maximum number of iterations Tmax, γ, ζ, etc;
t=0;
while (t<Tmax)
Identify the elite pollen Felite(t) in current iteration and the elite pollen Felite(t-1) in previous iteration;
  for i=1,2…,Np
    if rand>P
      Perform global search by formula (27);
      if rand<Pm
      Mutate the position of pollen i by formula (34);
        for j=1,2…,Nc (The dimension of the control variable)
          if rand<cr||d=drand
          Cross the j-th position of pollen i by formula (35);
          else
          Randomly cross over the j-th position of pollen i;
        end
     else
     Perform local search by formula (31);
  end
  Record the best individual of the previous generation Felite(t-1);
Update overall pollen positions;
t=t+1;
end while
output the best control variable set;
```

TABLE II
NINE DIFFERENT COMBINATIONS

Cases	J_{fcost}	$J_{emission}$	$J_{cost\text{-}vp}$	J_{ploss}	J_{VD}	Test systems
Case 1	✓			✓		IEEE 30
Case 2	✓	✓				
Case 3			✓	✓		
Case 4		✓		✓		
Case 5	✓	✓		✓		
Case 6				✓	✓	
Case 7	✓	✓				IEEE 57
Case 8	✓			✓		
Case 9	✓			✓		IEEE 118
Case 10	✓	✓				

Fig. 4 shows the structure of the IEEE118 standard test system. The system contains a set of 128-dimensional control variables, 54 generators and 9 transformers. The voltage of PV node is limited to 0.9-1.1 p.u. The range of shunt capacitor and transformer tap is the same as that of IEEE57.

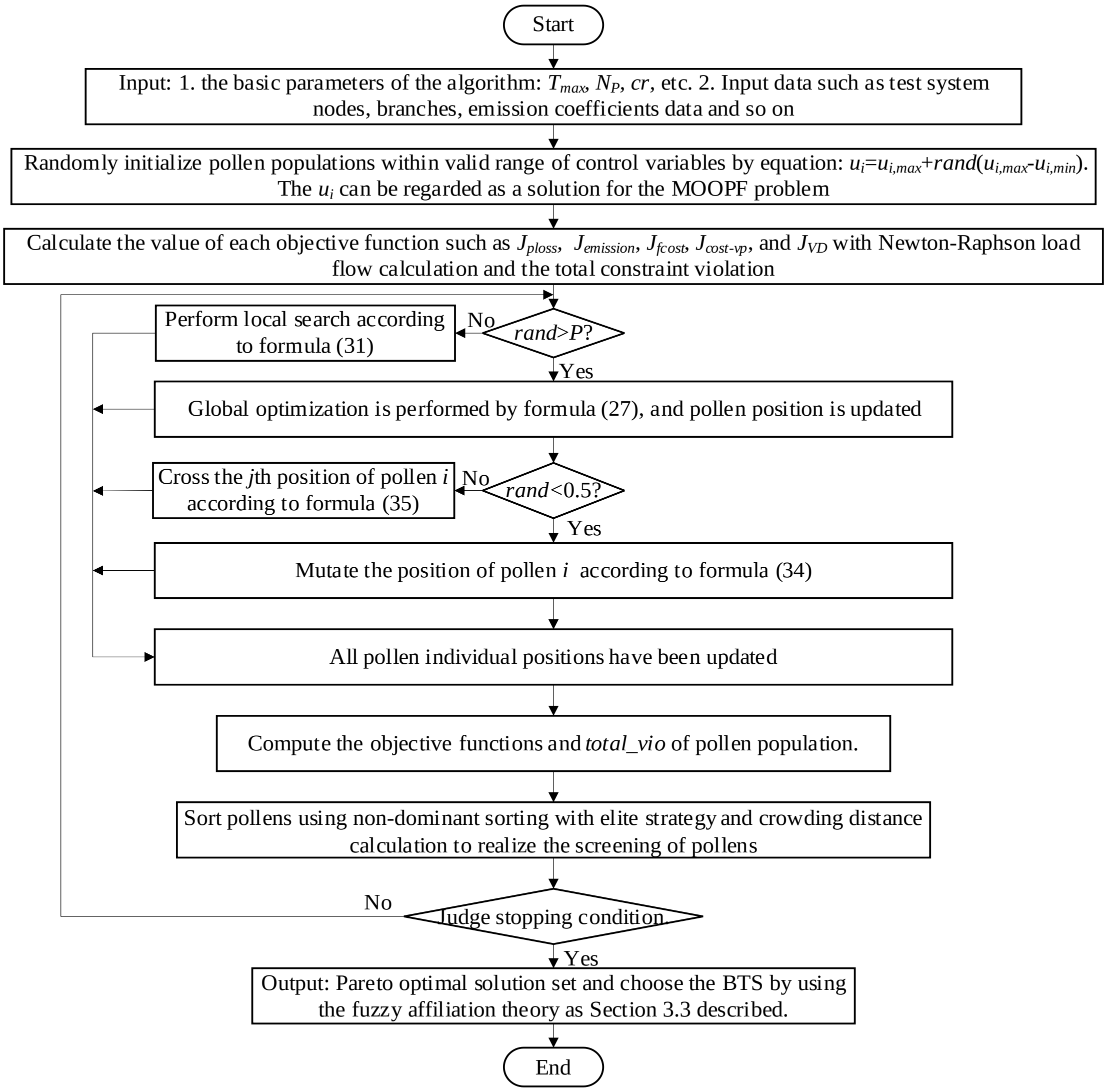

Fig. 1.the process of dealing with the MOOPF problem

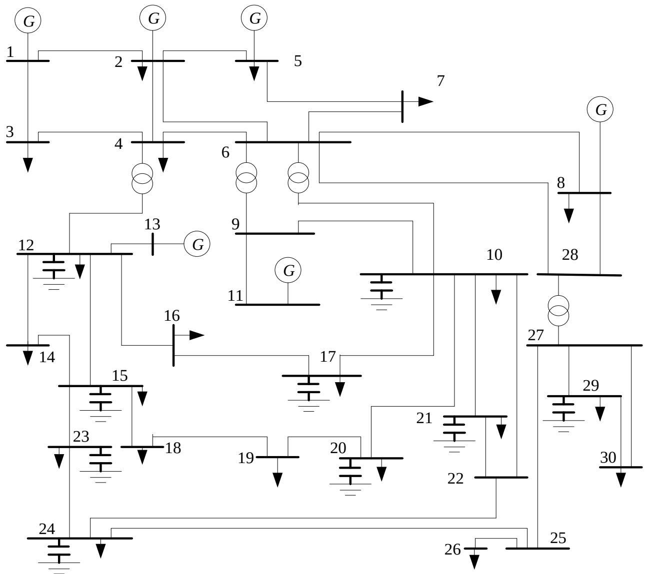

Fig. 2.the structure of the IEEE30 standard test system

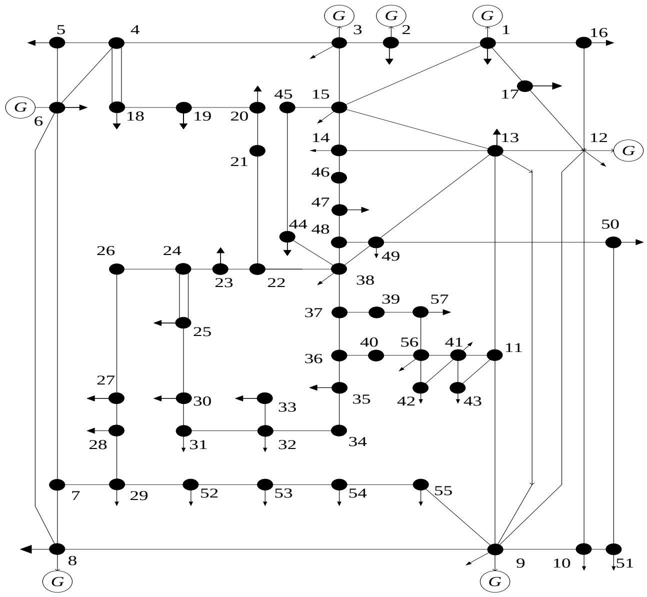

Fig. 3.the structure of the IEEE57 standard test system

B. Algorithm Parameters

Whether the parameter selection is appropriate or not will directly affect the results of the algorithm optimization, so it is necessary to adjust the algorithm parameters through experiments to optimize the efficiency of the algorithm.

Taking the combination of J_{ploss} and J_{fcost} on IEEE 30 standard test system as an example, the dual-objective experiments with a population size of 100 and different iterations from 100 to 500 are performed respectively. Fig. 5 shows the Pareto fronts obtained by different iterations. As can be seen from Fig. 5, the PFs obtained by iteration 100 generation is the worst, and the Pareto fronts obtained by 300, 400, and 500 iterations are well distribute. Considering comprehensively, it is determined that the number of iterations T_{max} of 300 is considered optimal. Fig. 6 shows the experimental results of 300 iterations with different population sizes N_P [30, 50, 100, 150]. It can be seen from Fig. 6 that the experimental results with population sizes of 100 and 150 are the best. In order to reduce the running time of the program, the population size N_P of the algorithm is determined to be 100. The detailed parameters of the algorithms are summarized in TABLE III.

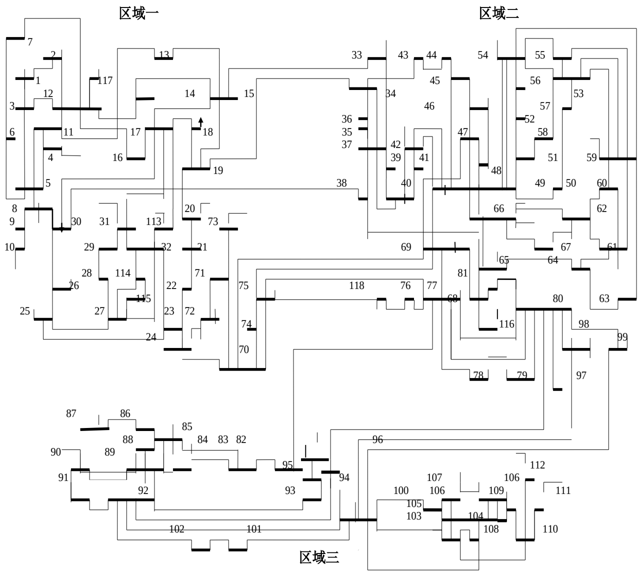

Fig. 4.the structure of the IEEE118 standard test system

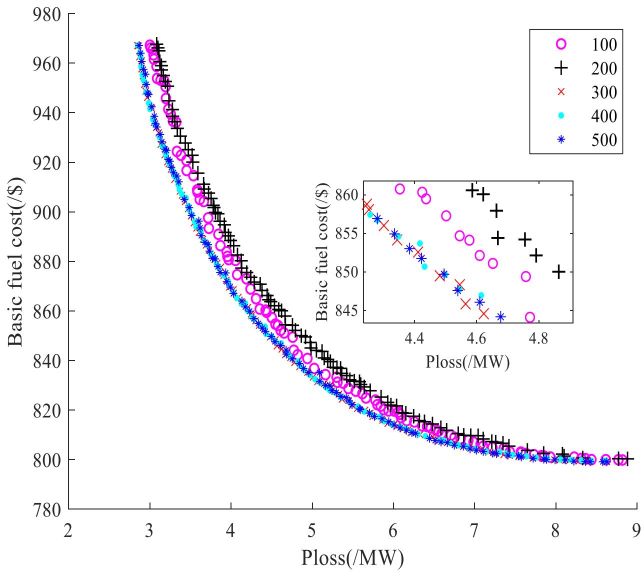

Fig. 5.PFs in different T_{max} with N_P of 100

C. IEEE30-bus System

The MOOPF cases 1-6 are carried out on the IEEE30 standard test system.

1) Case 1

In case 1, the basic fuel cost and active power loss are optimized by three algorithms simultaneously. The Pareto fronts are shown in Fig. 7. As can be seen in Fig. 7 that the Pareto front obtained by MHFPA is more uniform and continuous. TABLE III shows the 24-dimension control variables obtained by the three algorithms and the BTS solutions obtained based on equation (26). Among them, the BTS obtained by MHFPA algorithm includes the fuel cost of 833.1646 \$/h and the active power loss of 5.0266 MW, which are all less than the BTS obtained by MOPSO and NSGA-II algorithm. Furthermore, TABLE IV shows the BTS of Case 1 obtained by different methods proposed by various scholars in recent years. By comparing with other literatures, it further illustrates the superiority of the MHFPA algorithm dealing with the MOOPF problem.

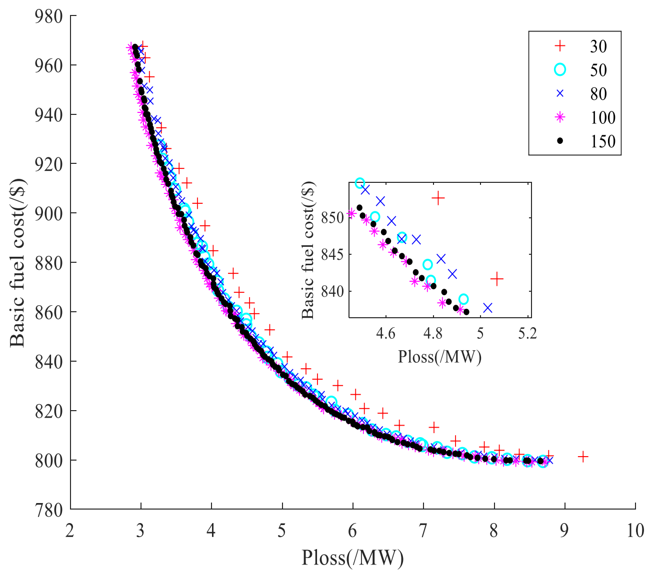

Fig. 6.PFs in different N_P with T_{max} of 300

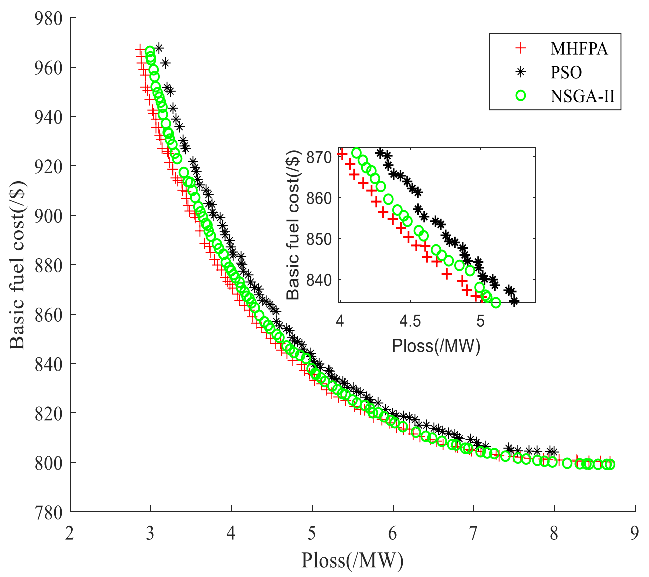

Fig. 7.PFs of Case 1

2) Case 2

In Case 2, the MOPSO, NSGA-II and MHFPA algorithms are used to optimize fuel cost and emission simultaneously, and the obtained BTS and its corresponding control variables are shown in TABLE VI. It can be seen from TABLE VI that the BTS obtained by MHFPA with 831.6277 \$/h of fuel cost and 0.2468 ton/h of emission dominant the ones obtained by MOPSO and NSGA-II approaches. Fig. 8 shows the Pareto fronts obtained by using three algorithms. It can be seen from Fig. 8 that the three algorithms can obtain the Pareto fronts.

TABLE III
THE DETAIL PARAMETERS OF THE ALGORITHMS

Methods	Parameters	Case1~Case6	Case7	Case8	Case9~10
MHFPA	Population size N_P	100	100	100	100
	Maximum Iteration T_{max}	300	500	500	500
	Switch probability P_{max}/P_{min}	0.8/0.2	0.8/0.2	0.8/0.2	0.8/0.2
	crossover constant cr	0.8	0.8	0.8	0.8
	Real constant factor Ψ_{max}/Ψ_{min}	0.8/0.2	0.8/0.2	0.8/0.2	0.8/0.2
	λ	1.5	1.5	1.5	1.5
MOPSO	Population size N_P	100	100	100	-
	Maximum Iteration T_{max}	300	500	500	-
	Inertia weight factor w_{max}/w_{min}	0.9/0.4	0.9/0.4	0.9/0.4	-
	Learning factor c_1/c_2	2/2	2/2	2/2	-
NSGA-II	Population size N_P	100	100	100	100
	Maximum Iteration T_{max}	300	500	500	500
	Mutation index/percentage	20/0.1	20/0.1	20/0.1	20/0.1
	Crossover index/percentage	20/0.1	20/0.1	20/0.1	20/0.1

TABLE IV
THE BEST SOLUTIONS OF CASE 1

control variables	MHFPA	NSGA-II	MOPSO
P_{Ge_2} (MW)	55.9490	51.1739	55.2040
P_{Ge_5}	31.8608	32.8422	33.2515
P_{Ge_8}	35.0000	34.8975	35.0000
P_{Ge_11}	24.1388	27.9880	28.8730
P_{Ge_13}	24.8255	23.6356	22.9246
V_{Ge_1} (p.u.)	1.1000	1.0999	1.0994
V_{Ge_2}	1.0907	1.0868	1.0913
V_{Ge_5}	1.0685	1.0524	1.0641
V_{Ge_8}	1.0773	1.0711	1.0766
V_{Ge_11}	1.0763	1.0982	1.0893
V_{Ge_13}	1.0962	1.0948	1.0413
T_{11} (p.u.)	1.0363	1.0006	1.0489
T_{12}	0.9150	0.9240	1.0513
T_{15}	1.0001	1.0094	1.0768
T_{36}	0.9697	0.9799	1.1000
Q_{Co_10}(p.u.)	0.0500	0.0247	0.0000
Q_{Co_12}	0.0335	0.0064	0.0170
Q_{Co_15}	0.0380	0.0320	0.0299
Q_{Co_17}	0.0500	0.0245	0.0000
Q_{Co_20}	0.0317	0.0203	0.0364
Q_{Co_21}	0.0500	0.0221	0.0439
Q_{Co_23}	0.0322	0.0344	0.0445
Q_{Co_24}	0.0496	0.0121	0.0471
Q_{Co_29}	0.0304	0.0191	0.0486
J_{fcost} ($/h)	**833.1646**	835.5818	840.0079
J_{ploss} (M W)	**5.0265**	5.0451	5.0257

TABLE V
COMPARISON OF LITERATURE IN CASE 1

Comparison	Fuel cost($/h)	Active power loss(MW)
MHFPA	**833.1646**	**5.0265**
NSGA-II	835.5818	5.0451
MOPSO	840.0079	5.0257
NMBAS[19]	831.1550	5.0707
MSA[31]	859.1915	4.5404
MOTLBO[10]	830.7813	5.2742
MODFA[23]	833.9365	4.9561
NSGA-III[23]	836.8076	5.1775

Although the gap is small, the Pareto front obtained by MHFPA algorithm is better than the other two algorithms according to the Pareto dominance rule.

TABLE VII shows the BTS of Case 2 obtained by different methods proposed by scholars in recent years. As can be seen from the table, the BTS obtained by MHFPA is superior to AGSO and ESDE algorithms, and is of the same priority as those obtained by MODFA and HFBA-COFS algorithms. All in all, the proposed MHFPA has competitive advantages compared with other algorithms.

3) Case 3

MOOPF case 3 optimizes J_{ploss} and $J_{cost\text{-}vp}$ concurrently, and the optimization results are shown in Fig. 9. It can be seen from Fig. 9 that the diversity of PF solution sets of the three algorithms are similar, but MHFPA has a better potential to obtain evenly distributed PF and the obtained PF is closer to the real front. TABLE VIII gives the BTS of Case 3 and its corresponding decision variables. Through data comparison, the BTS obtained by MHFPA algorithm, including fuel cost of 867.8158 $/h (valve point) and power loss of 5.6303 MW, is superior to the other two algorithms. In addition, the result is better than NHBA [8], which further strongly illustrates the effectiveness of the proposed method.

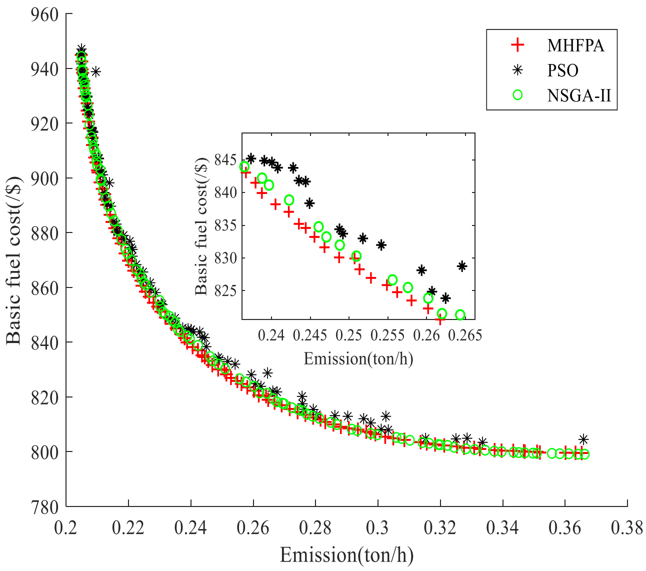

Fig. 8.PFs of Case 2

4) Case 4

In Case 4, power loss and emissions are optimized simultaneously, and the PFS obtained by the three algorithms are shown in Fig. 10. As we can see from Fig. 10, the red curve is closer to the real Pareto front, and the three curves are significantly different. Obviously, the simulation results obtained by the MHFPA algorithm are far superior to the other two algorithms, and regardless of the uniformity and diversity of the distribution, the performance of MHFPA is significantly better.

TABLE IX summarizes the experimental results of Case 4. It can be seen from the data that the emission data obtained by the three algorithms are the same, and the BTS of power loss and emission obtained by MHFPA algorithm are 2.8830 MW and 0.2054 ton/h respectively, which dominates MOPSO, NSGA-II and the MODFA algorithm in literature [23].

TABLE VI
THE BEST SOLUTIONS OF CASE 2

control variables	MHFPA	NSGA-II	MOPSO
P_{Ge_2} (MW)	58.3160	58.4837	62.1311
P_{Ge_5}	27.1604	27.3802	29.1484
P_{Ge_8}	35.0000	35.0000	35.0000
P_{Ge_11}	25.7353	27.1388	27.6693
P_{Ge_13}	26.0175	24.4721	18.5859
V_{Ge_1} (p.u.)	1.1000	1.0561	1.1000
V_{Ge_2}	1.0816	1.0501	1.0809
V_{Ge_5}	1.0545	1.0143	1.0280
V_{Ge_8}	1.0590	1.0169	1.0481
V_{Ge_11}	1.0472	1.0999	1.0736
V_{Ge_13}	1.0995	1.0562	1.0294
T_{11} (p.u.)	1.0675	1.0381	0.9000
T_{12}	0.9024	0.9001	1.0215
T_{15}	0.9902	0.9250	1.0002
T_{36}	0.9792	0.9531	0.9899
Q_{Co_10} (p.u.)	0.0318	0.0494	0.0293
Q_{Co_12}	0.0085	0.0499	0.0020
Q_{Co_15}	0.0023	0.0491	0.0111
Q_{Co_17}	0.0331	0.0395	0.0054
Q_{Co_20}	0.0500	0.0438	0.0313
Q_{Co_21}	0.0500	0.0130	0.0123
Q_{Co_23}	0.0500	0.0005	0.0440
Q_{Co_24}	0.0243	0.0413	0.0221
Q_{Co_29}	0.0397	0.0062	0.0242
J_{fcost} ($/h)	**831.6277**	833.2228	833.7139
$J_{emission}$ (ton/h)	**0.2468**	0.2470	0.2492

TABLE VII
COMPARISON OF LITERATURE IN CASE 2

Comparison	Fuel cost($/h)	Emission (ton/h)
MHFPA	**831.6277**	**0.2468**
NSGA-II	833.2228	0.2470
MOPSO	833.7139	0.2492
AGSO[9]	843.5473	0.2539
ESDE[33]	833.4743	0.2540
MODFA[23]	831.6652	0.2432
NSGA-III[23]	832.5323	0.2483
HFBA-COFS[24]	833.0155	0.2329
DE-PFA[24]	833.5200	0.2332

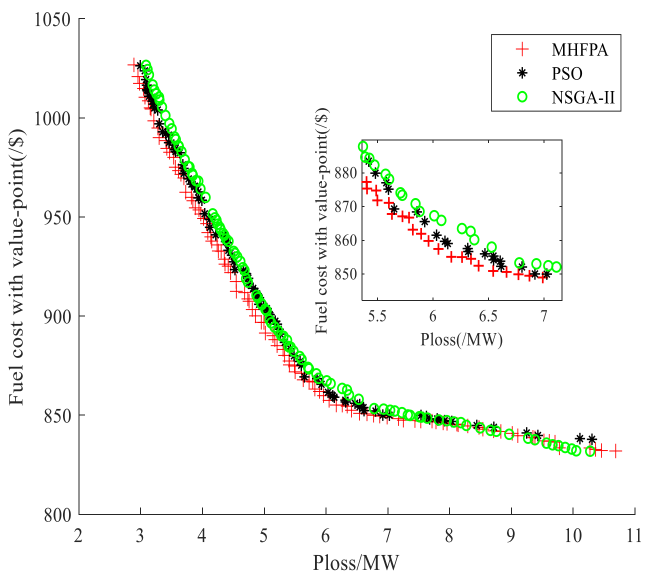

Fig. 9.PFs of Case 3

5) Case 5

Compared with dual-objective optimization, the simultaneous optimization of tri-objective will undoubtedly increase the difficulty of solving. In Case 5, the three conflicting objective functions of power loss, emission, and fuel cost are simultaneously optimized to illustrate the performance of MHFPA. Fig. 11 shows the optimal PF distributions of MHFPA, MOPSO, and NSGA-II. It again strongly illustrates that the PF of the MHFPA algorithm is more uniform than the other two algorithms, and the overall performance is the best.

TABLE VIII
THE BEST SOLUTIONS OF CASE 3

control variables	MHFPA	NSGA-II	MOPSO	NHBA[8]
P_{Ge_2} (MW)	46.5349	41.9419	44.6724	52.3984
P_{Ge_5}	34.8918	30.8531	32.7786	31.9677
P_{Ge_8}	34.9847	33.7896	34.0735	34.6347
P_{Ge_11}	25.6527	29.4862	25.4938	19.6335
P_{Ge_13}	12.0000	17.7004	18.5716	20.2407
V_{Ge_1} (p.u.)	1.1000	1.0801	1.1000	1.0992
V_{Ge_2}	1.0875	1.0623	1.0887	1.0992
V_{Ge_5}	1.0655	1.0427	1.0611	1.0697
V_{Ge_8}	1.0824	1.0483	1.0678	1.0804
V_{Ge_11}	1.1000	1.0888	1.0600	1.0972
V_{Ge_13}	1.0962	1.0752	1.0489	1.0707
T_{11} (p.u.)	1.0571	1.0416	1.0869	1.0257
T_{12}	0.9825	0.9130	0.9345	0.9754
T_{15}	1.0041	1.0150	1.0522	0.9818
T_{36}	1.0094	0.9725	1.0130	0.9868
Q_{Co_10}(p.u.)	0.0464	0.0395	0.0203	0.0276
Q_{Co_12}	0.0000	0.0400	0.0436	0.0277
Q_{Co_15}	0.0500	0.0486	0.0411	0.0242
Q_{Co_17}	0.0459	0.0438	0.0254	0.0256
Q_{Co_20}	0.0468	0.0054	0.0330	0.0397
Q_{Co_21}	0.0220	0.0318	0.0500	0.0310
Q_{Co_23}	0.0334	0.0439	0.0000	0.0315
Q_{Co_24}	0.0488	0.0218	0.0383	0.0269
Q_{Co_29}	0.0326	0.0040	0.0380	0.0205
$J_{fcost\text{-}vp}$ ($/h)	**867.8159**	868.5625	869.3050	868.9526
J_{ploss} (MW)	**5.6303**	5.8794	5.6504	5.6761

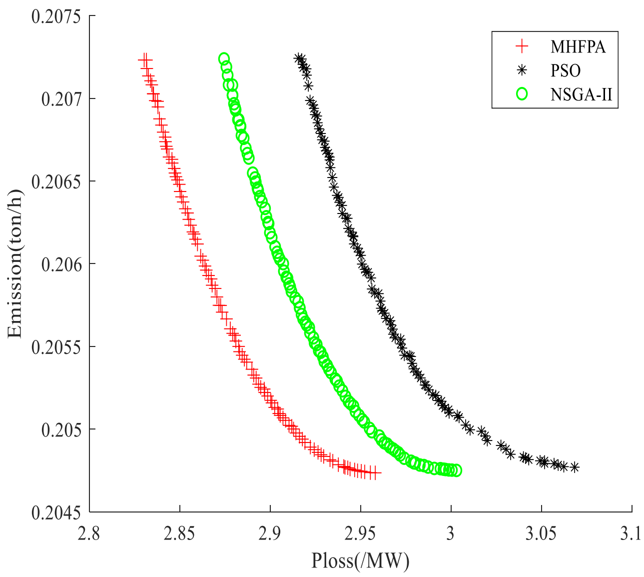

Fig. 10. PFs of Case 4

TABLE X shows the BTS obtained by the fuzzy affiliation theory. It can be seen from the results that the BTS solution of the MHFPA algorithm dominates the MOPSO and NSGA-II algorithms. Among them, the BTS of fuel cost, power loss and emission obtained by the MHFPA algorithm are 879.4391 \$/h, 3.9070 MW and 0.2167 ton/h, respectively. Compared with the MOFA-PFA in literature [5], the BTS of the MHFPA algorithm have superior J_{fcost} and J_{ploss}, and the $J_{emission}$ is almost the same.

6) Case 6

The voltage deviation plays a vital role in the normal operation of the power system. If the voltage fluctuation of the system is too large, it may cause the phenomenon of the frequency instability of the system, and even lead to the breakdown of the power system in serious cases.

Case 6 optimizes the voltage deviation and power loss on the IEEE30 standard system at the same time. Fig. 12 shows the Pareto fronts obtained by the MHFPA, MOPSO and NSGA-II algorithms, and TABLE XI lists the detailed simulation results. According to the above results, the BTS of power loss and voltage deviation obtained by MHFPA algorithm are 3.0366 MW and 0.5267 respectively, which are superior to MOPSO and NSGA-II algorithms.

TABLE IX
THE BEST SOLUTIONS OF CASE 4

control variables	MHFPA	NSGA-II	MOPSO	MODFA[23]
P_{Ge_2} (MW)	74.2742	73.9428	74.0868	74.1405
P_{Ge_5}	49.9979	49.9999	50.0000	49.9999
P_{Ge_8}	34.9978	34.9947	35.0000	35.0000
P_{Ge_11}	30.0000	29.9998	30.0000	29.9998
P_{Ge_13}	40.0000	39.9990	40.0000	39.9999
V_{Ge_1} (p.u.)	1.0999	1.0921	1.1000	1.1000
V_{Ge_2}	1.0967	1.0854	1.1000	1.0967
V_{Ge_5}	1.0789	1.0672	1.1000	1.0784
V_{Ge_8}	1.0860	1.0742	1.0942	1.0860
V_{Ge_11}	1.0998	1.0996	1.1000	1.0999
V_{Ge_13}	1.0999	1.0999	1.1000	1.1000
T_{11}(p.u.)	1.0580	1.0176	1.0735	1.0549
T_{12}	0.9000	0.9160	0.9000	0.9007
T_{15}	0.9873	0.9712	0.9948	0.9878
T_{36}	0.9724	0.9639	0.9820	0.9725
Q_{Co_10}(p.u.)	0.0490	0.0391	0.0500	0.0480
Q_{Co_12}	0.0491	0.0267	0.0500	0.0490
Q_{Co_15}	0.0432	0.0404	0.0500	0.0444
Q_{Co_17}	0.0492	0.0497	0.0500	0.0495
Q_{Co_20}	0.0378	0.0325	0.0406	0.0373
Q_{Co_21}	0.0497	0.0500	0.0500	0.0500
Q_{Co_23}	0.0243	0.0362	0.0184	0.0231
Q_{Co_24}	0.0499	0.0497	0.0500	0.0500
Q_{Co_29}	0.0215	0.0245	0.0242	0.0222
$J_{emission}$ (ton/h)	**0.2054**	0.2054	0.2054	0.2054
J_{ploss} (MW)	**2.8830**	2.9298	2.9741	2.8841

TABLE X
THE BEST SOLUTIONS OF CASE 5

control variables	MHFPA	NSGA-II	MOPSO	MOFA-PFA [5]
P_{Ge_2} (MW)	63.8440	62.4853	63.9466	57.8900
P_{Ge_5}	38.1260	42.9497	39.5116	36.2900
P_{Ge_8}	34.7302	34.0751	34.5969	35.0000
P_{Ge_11}	30.0000	28.6734	27.7020	29.2710
P_{Ge_13}	33.8685	30.4050	33.8351	40.0000
V_{Ge_1} (p.u.)	1.0979	1.0516	1.1000	1.0985
V_{Ge_2}	1.0896	1.0396	1.0937	1.0869
V_{Ge_5}	1.0705	1.0154	1.0849	1.0625
V_{Ge_8}	1.0836	1.0295	1.0917	1.0767
V_{Ge_11}	1.0936	1.0856	1.0913	1.0857
V_{Ge_13}	1.1000	1.0398	1.0974	1.0386
T_{11} (p.u.)	1.0180	1.0240	1.1000	1.0860
T_{12}	0.9592	0.9027	0.9290	0.9930
T_{15}	1.0222	0.9609	1.0262	1.0520
T_{36}	0.9786	0.9787	0.9802	1.0770
Q_{Co_10}(p.u.)	0.0319	0.0140	0.0046	0.0140
Q_{Co_12}	0.0000	0.0229	0.0102	0.0220
Q_{Co_15}	0.0500	0.0266	0.0500	0.0080
Q_{Co_17}	0.0397	0.0425	0.0451	0.0250
Q_{Co_20}	0.0137	0.0180	0.0337	0.0390
Q_{Co_21}	0.0500	0.0353	0.0328	0.0270
Q_{Co_23}	0.0500	0.0031	0.0305	0.0100
Q_{Co_24}	0.0389	0.0241	0.0500	0.0170
Q_{Co_29}	0.0369	0.0233	0.0500	0.0500
$J_{emission}$ (ton/h)	**0.2167**	0.2183	0.2178	0.2165
J_{ploss} (MW)	**3.9070**	4.2617	4.0056	4.2179
J_{fcost}(\$/h)	**879.4391**	885.1467	879.9349	879.9100

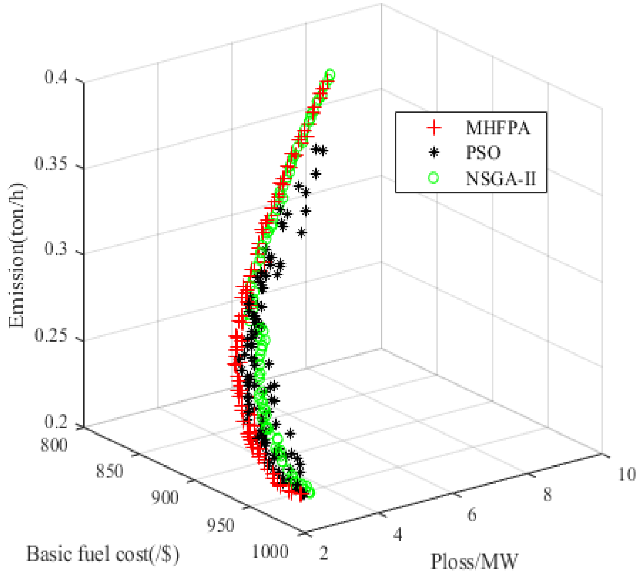

Fig. 11. PFs of Case 5

TABLE XI
THE BEST SOLUTIONS OF CASE 6

control variables	MHFPA	NSGA-II	MOPSO
P_{Ge_2} (MW)	80.0000	79.9842	80.000
P_{Ge_5}	49.9969	49.9999	5.0000
P_{Ge_8}	34.9826	34.9931	35.0000
P_{Ge_11}	29.9864	29.9996	30.0000
P_{Ge_13}	39.9388	40.0000	40.0000
V_{Ge_1} (p.u.)	1.1000	1.0999	1.1000
V_{Ge_2}	1.0949	1.0968	1.1000
V_{Ge_5}	1.0729	1.0813	1.0854
V_{Ge_8}	1.0798	1.0853	1.1000
V_{Ge_11}	1.0063	1.0682	1.1000
V_{Ge_13}	1.0348	1.0262	1.0224
T_{11}(p.u.)	1.0934	1.1000	1.1000
T_{12}	0.9771	1.0346	1.1000
T_{15}	1.0727	1.0662	1.0685
T_{36}	1.0373	1.0357	1.0521
Q_{Co_10} (p.u.)	0.0456	0.0070	0.0000
Q_{Co_12}	0.0222	0.0260	0.0000
Q_{Co_15}	0.0368	0.0243	0.0000
Q_{Co_17}	0.0324	0.0461	0.0261
Q_{Co_20}	0.0500	0.0369	0.0500
Q_{Co_21}	0.0500	0.0245	0.0500
Q_{Co_23}	0.0245	0.0405	0.0500
Q_{Co_24}	0.0500	0.0432	0.0500
Q_{Co_29}	0.0208	0.0201	0.0193
J_{VD}	**0.5267**	0.5661	0.6117
J_{ploss} (MW)	**3.0366**	3.0339	3.0843

D. IEEE57-bus System

Two dual-objective MOOPF optimization experiments are carried out on IEEE57 standard test system. Compared with the IEEE30 system, the system is harder to find the best solution, and it is also a test of the proposed algorithm.

1) Case 7

Simultaneous optimization of total fuel cost functions and emission functions is the core of Case 7. TABLE XII lists the control variables and BTS obtained by the three methods. Among them, the BTS of fuel costs and emissions obtained by the MHFPA algorithm are 42939.6926 \$/h and 1.3033 ton/h, respectively. It still can be concluded from the table that MHFPA obtains the best results. The Pareto optimal fronts obtained by MHFPA, MOPSO and NSGA-II are shown in Fig. 13. It can be clearly seen from the figure that MHFPA obtains a uniformly distributed Pareto solution set, and a better Pareto front than the other two methods.

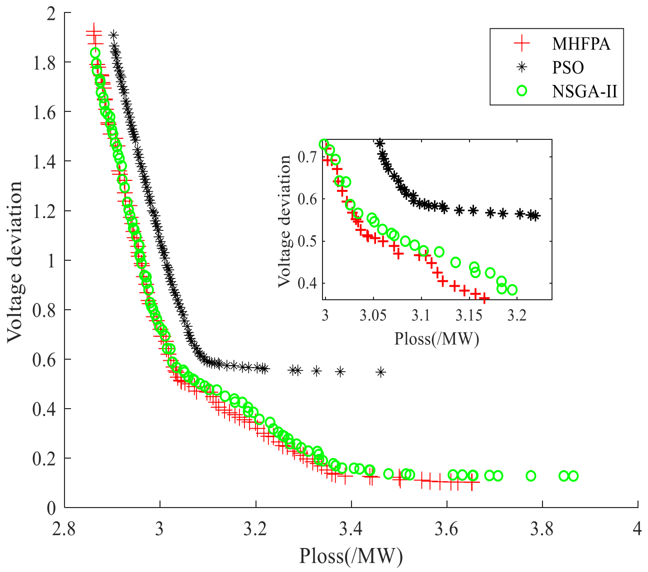

Fig. 12. PFs of Case 6

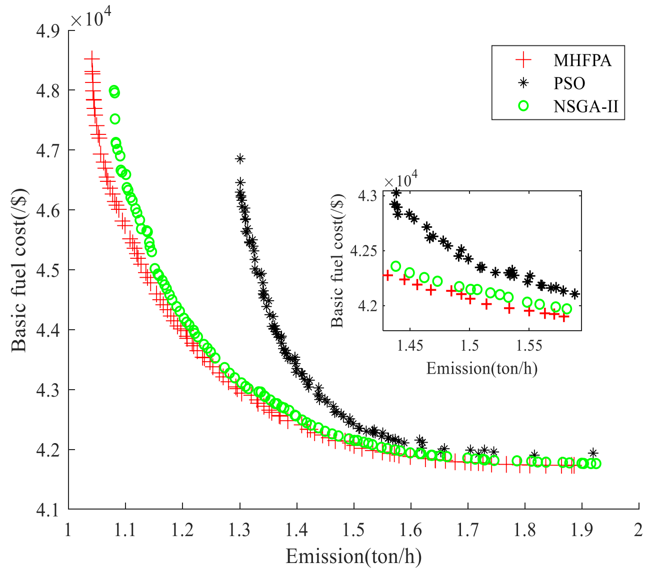

Fig. 13. PFs of Case 7

2) Case 8

In case 8, the total fuel cost and power loss are considered concurrently. The experimental results are shown in Fig. 14. It can be clearly seen from the figure that MHFPA has better Pareto front than MOPSO and NSGA-II, and the distribution is more uniform and continuous. TABLE XII shows the BTS and control variables of the three algorithms and MOIBA in the literature [6] in case 8. Among them, the BTS calculated by the MHFPA algorithm includes the fuel cost of 42092.6602 \$/h and the power loss of 10.8947 MW. The comparison shows that MHFPA has obtained the least fuel cost and network loss.

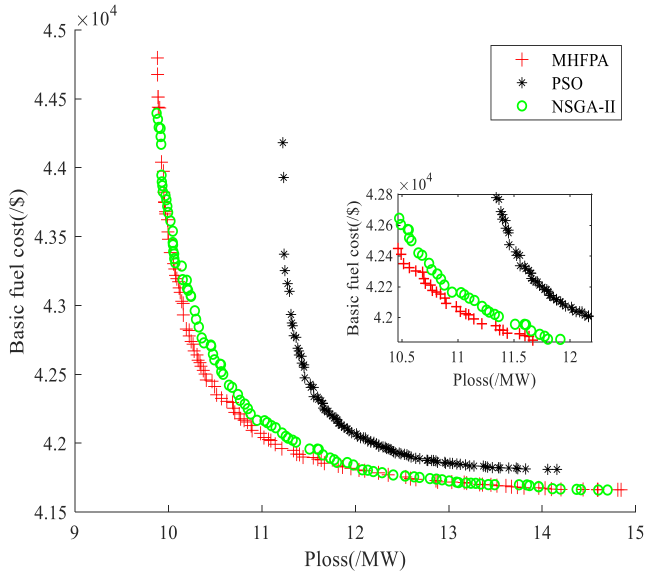

Fig. 14. PFs of Case 8

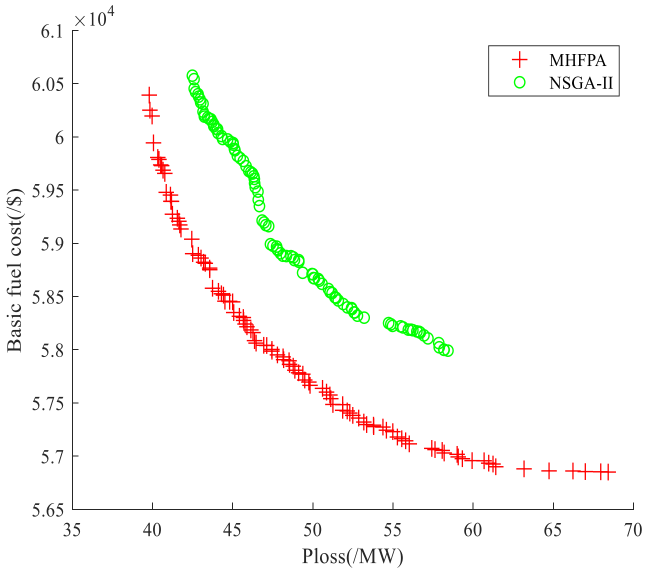

Fig. 15. PFs of Case 9

E. IEEE118-bus System

The IEEE118-bus test system is more complicated than the above two systems in terms of the system structure and the dimensionality of control variables. In recent years, few scholars have used the 118-bus test system for testing, and many algorithms can hardly find well-distributed Pareto fronts in this system, such as MOPSO.

1) Case 9

In case 9, the basic fuel cost and loss are optimized at the same time. As the PF front obtained by MOPSO method in solving this MOOPF case is extremely scattered and disorderly, it is not presented in this paper. Fig. 15 shows that the PF obtained by the MHFPA algorithm has a better

TABLE XII
THE BEST SOLUTIONS OF CASE 7 AND CASE 8

control variables	Case 7				Case 8			
	MHFPA	NSGA-II	MOPSO	MPIO-COSR[22]	MHFPA	NSGA-II	MOPSO	MOIBA[6]
P_{Ge_2} (MW)	100.0000	99.9706	97.2820	100.0000	76.1758	59.0801	86.1457	53.4086
P_{Ge_3}	85.6281	78.4012	64.4218	85.5144	61.7668	66.9557	66.2748	62.6900
P_{Ge_6}	99.9643	100.0000	100.000	99.7250	100.0000	98.8679	98.2139	89.8593
P_{Ge_8}	342.7870	344.2919	311.3586	348.8135	362.0245	364.6732	349.5353	377.9932
P_{Ge_9}	99.6791	99.9012	100.0000	98.8729	98.5667	99.9354	99.9977	99.9232
P_{Ge_12}	327.3909	326.2140	410.0000	306.1420	410.0000	410.0000	409.8576	410.0000
V_{Ge_1} (p.u.)	1.0296	0.9850	1.1000	1.0793	1.0687	1.0561	1.1000	1.0536
V_{Ge_2}	1.0230	0.9770	1.1000	1.0768	1.0626	1.0534	1.1000	1.0467
V_{Ge_3}	1.0163	0.9903	1.1000	1.0716	1.0515	1.0578	1.1000	1.0436
V_{Ge_6}	1.0297	1.0243	1.1000	1.0903	1.0609	1.0737	1.1000	1.0521
V_{Ge_8}	1.0330	1.0509	1.1000	1.0879	1.0664	1.0825	1.1000	1.0613
V_{Ge_9}	1.0140	1.0335	1.1000	1.0651	1.0517	1.0707	1.1000	1.0481
V_{Ge_12}	1.0204	1.0177	1.1000	1.0460	1.0490	1.0592	1.1000	1.0337
T_{19} (p.u.)	0.9000	1.0424	1.0528	1.0312	0.9817	1.0956	0.9279	1.0350
T_{20}	1.0974	1.0300	1.0688	1.0520	1.0399	1.0725	1.1000	0.9496
T_{31}	1.0878	1.0110	0.9000	0.9862	1.0405	1.0263	1.1000	0.9837
T_{35}	0.9855	1.0327	1.0904	0.9439	0.9843	1.0347	0.9936	1.0267
T_{36}	1.1000	0.9666	1.0244	1.0043	1.0269	1.0707	0.9851	1.0055
T_{37}	1.0716	0.9481	1.0899	1.0161	1.0514	1.0031	1.0590	1.0597
T_{41}	0.9620	0.9377	1.1000	1.0041	0.9980	0.9980	1.1000	0.9682
T_{46}	1.0112	1.0207	0.9000	1.0109	0.9368	0.9689	0.9367	0.9558
T_{54}	0.9181	0.9704	0.9511	0.9165	0.9002	1.0008	0.9362	0.9893
T_{58}	0.9395	0.9395	1.0334	0.9596	0.9494	0.9742	1.0252	0.9281
T_{59}	0.9060	0.9641	0.9861	0.9588	0.9375	0.9848	1.1000	0.9192
T_{65}	0.9306	0.9724	1.0415	0.9773	0.9424	0.9927	1.0408	0.9525
T_{66}	0.9000	0.9000	0.9758	0.9573	0.9035	0.9549	1.0021	0.9441
T_{71}	0.9529	0.9575	1.1000	0.9922	0.9589	0.9495	1.0810	0.9527
T_{73}	0.9974	1.0101	0.9839	1.0562	0.9964	0.9527	1.1000	0.9421
T_{76}	0.9502	0.9887	0.9713	0.9812	1.0624	0.9931	0.9407	1.0606
T_{80}	0.9333	0.9783	1.0492	1.0582	1.0038	1.0161	1.0920	0.9688
Q_{Co_18} (p.u.)	0.2106	0.2543	0.0000	0.2283	0.2062	0.2982	0.0955	0.2343
Q_{Co_25}	0.1569	0.2111	0.1761	0.1166	0.1108	0.1826	0.1674	0.1310
Q_{Co_53}	0.1258	0.1597	0.3000	0.1542	0.1713	0.1564	0.1607	0.1876
J_{fcost} (\$/h)	**42939.6926**	43013.9664	42618.6901	43131.2743	**42092.6602**	42165.6695	42242.0329	42098.7213
$J_{emission}$ (ton/h)	**1.3033**	1.3153	1.4664	1.2314	-	-	-	-
J_{ploss}(MW)	-	-	-	-	**10.8947**	10.9477	11.6702	11.4759

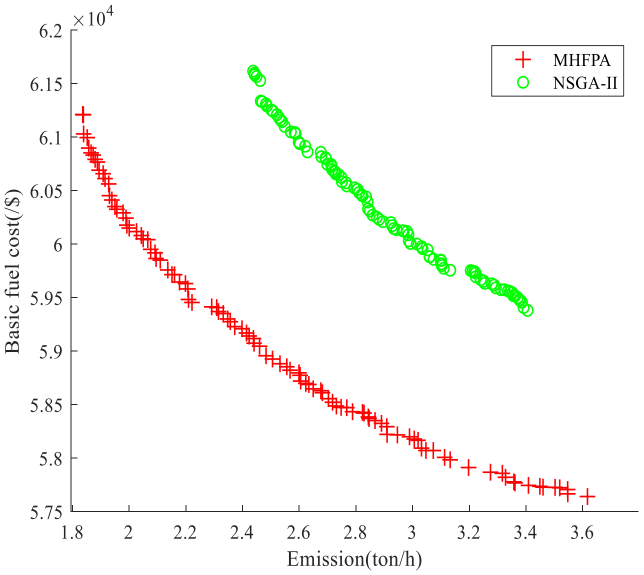

Fig. 16. PFs of Case 10

distribution uniformity, and its performance has obvious advantages compared with the NSGA-II method. The BTS of MHFPA, NSGA-II are given in TABLE XV. It can be seen from TABLE XV that the BTS searched by MHFPA algorithm, including the fuel cost of 58061.7674 \$/h and the power loss of 46.4566 MW dominate other algorithms. TABLE XIII shows the BTS of Case 9 obtained by different methods proposed by scholars in recent years. As we can see from the data in the table, even in the face of large-scale system, the proposed method is still reliable and has a large competitive edge.

TABLE XIII
COMPARISON OF LITERATURE IN CASE 9

Algorithms	Fuel cost(\$/h)	Active power loss(MW)
MHFPA	**58061.7674**	**46.4566**
NSGA-II	58991.1959	47.3533
HFBA-COFS[24]	59624.0613	61.0362
MONIWCA[7]	58258.0000	49.7308

TABLE XIV
COMPARISON OF LITERATURE IN CASE 10

Algorithms	Fuel cost(\$/h)	Emission (ton/h)
MHFPA	**59455.5016**	**2.2220**
NSGA-II	60271.7117	2.8592
MODFA[23]	59590.5889	2.4971

2) Case 10

Case 10 also considers optimizing emissions and fuel costs at the same time on the IEEE118-bus system. It can be seen from Fig. 16 that the Pareto optimal solutions obtained by the proposed MHFPA are diverse, uniform, and closer to the real Pareto front. Experimental data are summarized in TABLE XIV and TABLE XVIII, from which we can see that BTS obtained by MHFPA includes 59455.5016\$/h fuel cost and

TABLE XV
THE BEST SOLUTIONS OF CASE 9

control variables	MHFPA	NSGA-II	control variables	MHFPA	NSGA-II
P_{Ge_4} (MW)	9.6456	13.0025	V_{Ge_26}	1.0173	1.0060
P_{Ge_6}	5.0919	17.3434	V_{Ge_27}	0.9992	0.9919
P_{Ge_8}	5.1944	11.1114	V_{Ge_31}	1.0097	1.0015
P_{Ge_10}	167.2912	199.3599	V_{Ge_32}	1.0372	0.9970
P_{Ge_12}	270.6777	246.3299	V_{Ge_34}	1.0392	0.9925
P_{Ge_15}	12.4749	10.5972	V_{Ge_36}	1.0065	0.9792
P_{Ge_18}	95.6150	92.3543	V_{Ge_40}	1.0024	0.9810
P_{Ge_19}	8.0322	6.8328	V_{Ge_42}	1.0114	1.0162
P_{Ge_24}	5.2829	6.8095	V_{Ge_46}	1.0221	1.0044
P_{Ge_25}	101.7980	111.5554	V_{Ge_49}	1.0048	0.9942
P_{Ge_26}	257.6937	253.7497	V_{Ge_54}	1.0030	1.0014
P_{Ge_27}	8.1901	13.4359	V_{Ge_55}	1.0014	0.9943
P_{Ge_31}	10.8714	8.9979	V_{Ge_56}	0.9993	1.0101
P_{Ge_32}	73.2077	28.7453	V_{Ge_59}	1.0050	1.0170
P_{Ge_34}	8.0000	8.8022	V_{Ge_61}	0.9966	1.0060
P_{Ge_36}	28.5055	41.1790	V_{Ge_62}	1.0177	1.0307
P_{Ge_40}	11.1848	17.9461	V_{Ge_65}	1.0261	1.0052
P_{Ge_42}	8.0222	9.5616	V_{Ge_66}	1.0146	1.0270
P_{Ge_46}	39.9499	35.3158	V_{Ge_69}	1.0023	1.0412
P_{Ge_49}	244.7500	231.4941	V_{Ge_70}	1.0395	1.0098
P_{Ge_54}	237.8432	249.4761	V_{Ge_72}	1.0186	1.0304
P_{Ge_55}	31.6294	48.2464	V_{Ge_73}	0.9750	1.0195
P_{Ge_56}	27.9347	30.5565	V_{Ge_74}	0.9928	0.9798
P_{Ge_59}	193.9127	138.4071	V_{Ge_76}	1.0250	1.0090
P_{Ge_61}	193.6305	132.6099	V_{Ge_77}	1.0463	1.0152
P_{Ge_62}	25.1129	30.6604	V_{Ge_80}	1.0157	1.0171
P_{Ge_65}	235.1790	255.4845	V_{Ge_85}	0.9978	0.9838
P_{Ge_66}	203.4983	215.9670	V_{Ge_87}	0.9298	0.9320
P_{Ge_69}	39.6294	71.9656	V_{Ge_89}	1.0125	1.0042
P_{Ge_70}	10.1322	15.7263	V_{Ge_90}	1.0049	1.0045
P_{Ge_72}	7.6457	16.4490	V_{Ge_91}	0.9981	1.0173
P_{Ge_73}	5.1153	7.0109	V_{Ge_92}	1.0122	1.0157
P_{Ge_74}	77.3687	40.5503	V_{Ge_99}	0.9935	1.0181
P_{Ge_76}	27.0217	30.3313	V_{Ge_100}	1.0143	1.0062
P_{Ge_77}	211.7708	203.0969	V_{Ge_103}	1.0089	0.9977
P_{Ge_80}	45.3373	69.8253	V_{Ge_104}	0.9955	0.9878
P_{Ge_85}	10.1467	10.0146	V_{Ge_105}	0.9877	0.9947
P_{Ge_87}	100.2394	100.1037	V_{Ge_107}	0.9503	0.9758
P_{Ge_89}	52.5193	73.3158	V_{Ge_110}	1.0036	1.0514
P_{Ge_90}	9.8722	10.9635	V_{Ge_111}	1.0147	1.0671
P_{Ge_91}	20.1829	20.4534	V_{Ge_112}	0.9988	1.0590
P_{Ge_92}	123.5968	109.6392	V_{Ge_113}	1.0346	0.9984
P_{Ge_99}	100.9328	101.1900	V_{Ge_116}	1.0022	1.0306
P_{Ge_100}	103.8077	104.6278	T_8 (p.u.)	1.0356	0.9927
P_{Ge_103}	8.5464	12.0017	T_{32}	0.9346	1.0571
P_{Ge_104}	29.6680	34.4245	T_{36}	0.9243	1.0663
P_{Ge_105}	26.0217	37.8337	T_{51}	0.9659	1.0180
P_{Ge_107}	8.8591	8.2530	T_{93}	1.0358	0.9476
P_{Ge_110}	25.5086	35.8354	T_{95}	1.0205	0.9826
P_{Ge_111}	26.5214	25.5422	T_{102}	0.9474	1.0424
P_{Ge_112}	27.4697	25.0449	T_{107}	1.0027	1.0055
P_{Ge_113}	25.9396	41.9077	T_{127}	0.9002	0.9550
P_{Ge_116}	25.0017	25.0739	Q_{Co_34} (p.u.)	0.0862	0.2460
V_{Ge_1} (p.u.)	1.0266	1.0022	Q_{Co_44}	0.1346	0.2467
V_{Ge_4}	1.0292	1.0066	Q_{Co_45}	0.2108	0.3000
V_{Ge_6}	1.0415	1.0188	Q_{Co_46}	0.0369	0.2763
V_{Ge_8}	1.0541	1.0445	Q_{Co_48}	0.0541	0.0886
V_{Ge_10}	1.0285	0.9991	Q_{Co_74}	0.2013	0.0603
V_{Ge_12}	1.0290	0.9829	Q_{Co_79}	0.0473	0.1521
V_{Ge_15}	1.0238	0.9871	Q_{Co_82}	0.01191	0.1141
V_{Ge_18}	1.0140	0.9852	Q_{Co_83}	0.0230	0.2910
V_{Ge_19}	1.0102	0.9849	Q_{Co_105}	0.2987	0.1459
V_{Ge_24}	1.0265	1.0237	Q_{Co_107}	0.3000	0.1512
V_{Ge_25}	0.9582	0.9865	Q_{Co_110}	0.2843	0.0230
			J_{fcost} ($/h)	**58061.7674**	58991.1959
			J_{ploss}(MW)	**46.4566**	47.3533

2.2220 ton/h emission, which is superior to NSGA-II and MODFA algorithm in literature [23].

Through the simulation experiments of Cases 1-10, we can find that the results of MHFPA also have a competitive advantage compared with many methods in literature.

F. Performance Evaluation

Spacing (SP) and hypervolume (HV) provide quantitative indicators for evaluating the quality of the PF solution sets obtained by different algorithms to deal with MOOPF

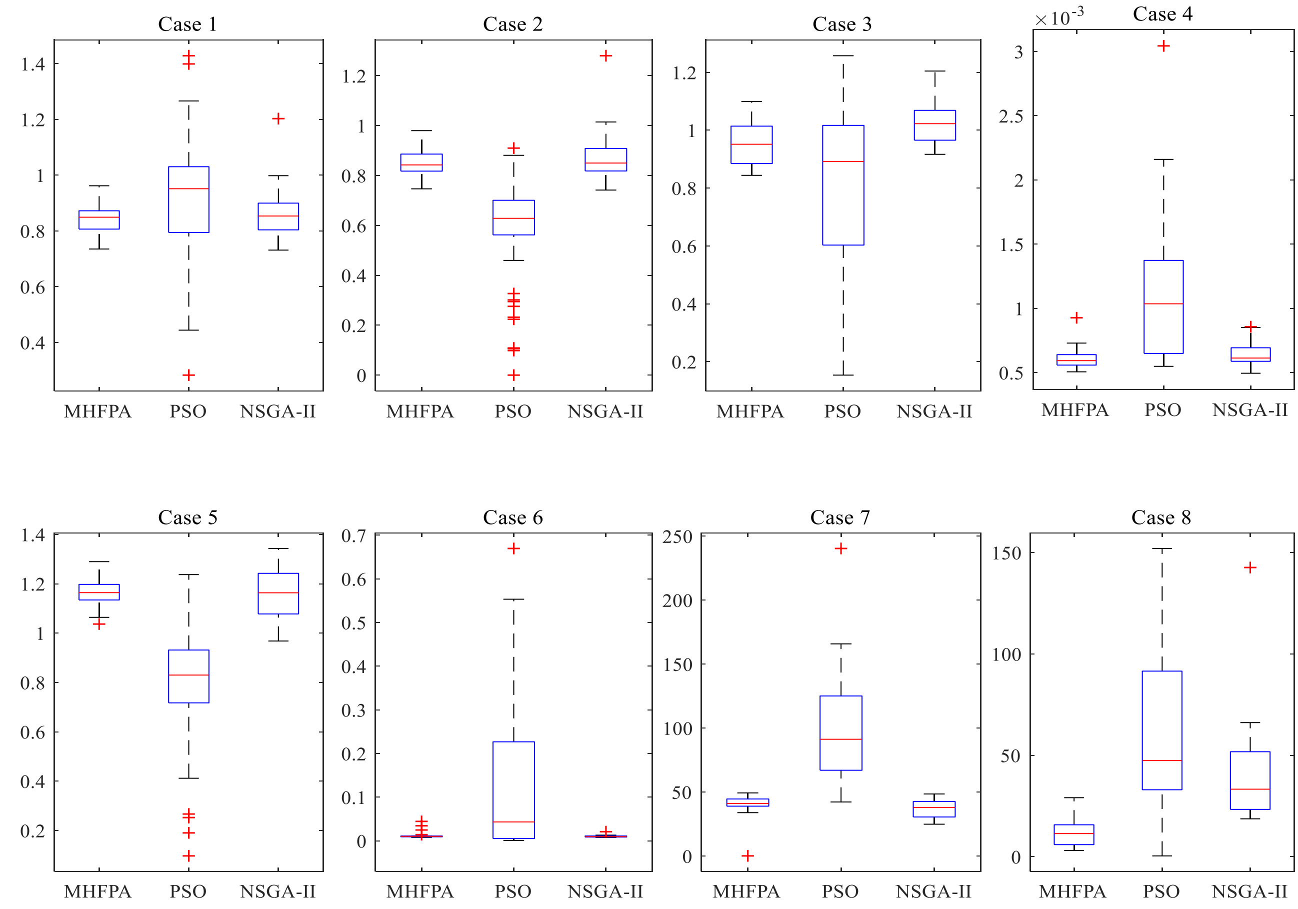

Fig. 17. Box plots of SP

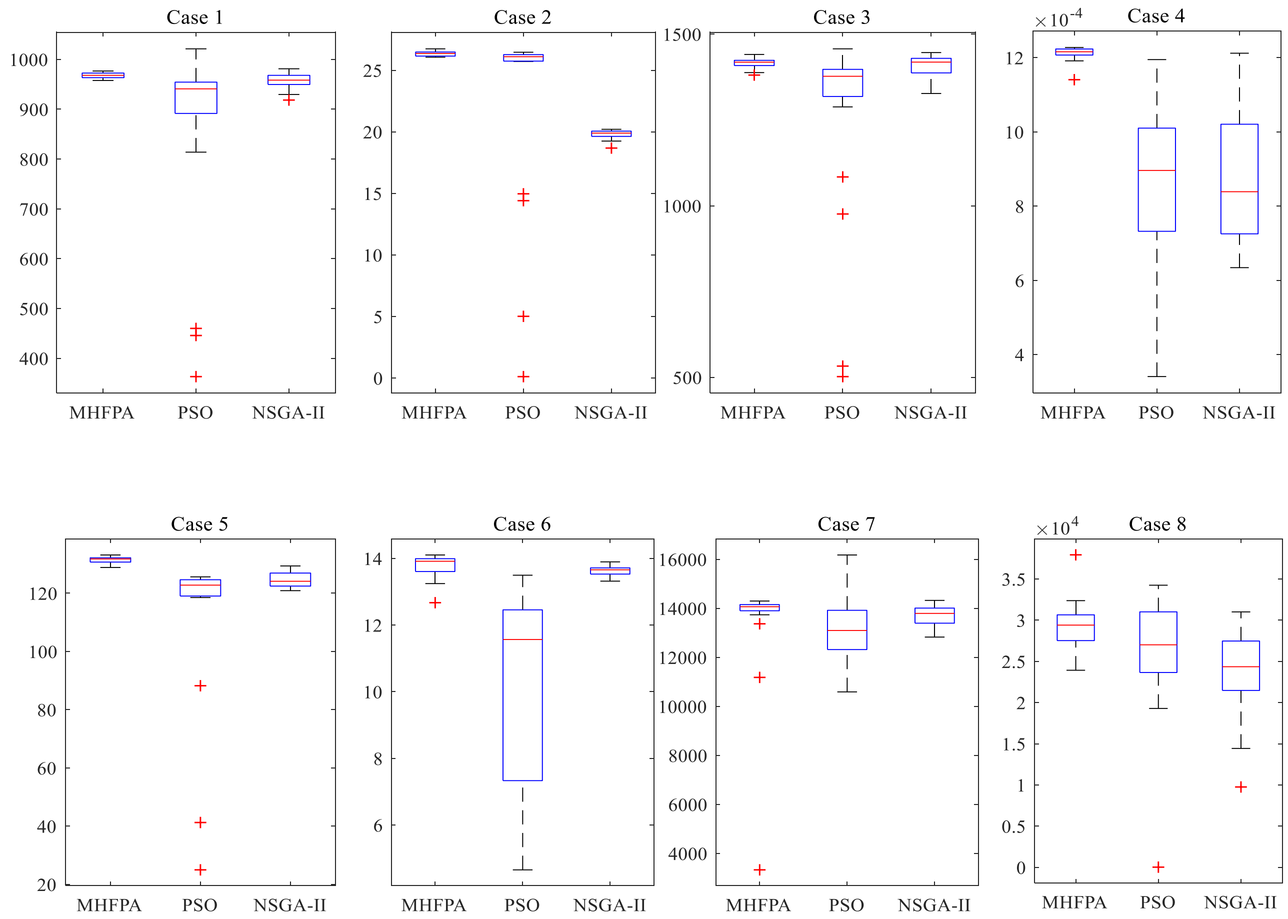

Fig. 18. Box plots of HV

TABLE XVI
DETAILED DATA OF THE BOX PLOT OF THE THREE ALGORITHMS

Indexes	Cases	MHFPA		MOPSO		NSGA-II	
		Mean	Deviation	Mean	Deviation	Mean	Deviation
SP	Case 1	0.8453	0.0550	0.9124	0.2782	0.8653	0.1009
	Case 2	0.8573	0.0571	0.5789	0.2154	0.8651	0.0845
	Case 3	0.9586	0.0809	0.8099	0.2846	1.0239	0.0719
	Case 4	0.0006	9.1E-05	0.0012	0.0008	0.0006	9.6E-05
	Case 5	1.1594	0.0606	0.7812	0.2896	1.1670	0.1006
	Case 6	0.0137	0.0096	0.1414	0.2081	0.0104	0.0029
	Case 7	37.2516	7.4955	100.9377	47.6488	39.5981	10.0045
	Case 8	12.1516	6.8862	63.0804	42.1731	41.5510	27.7388
HV	Case 1	968.0628	5.4799	858.6444	192.6302	956.9300	16.2336
	Case 2	26.3313	0.2155	22.4569	8.4844	19.8159	0.3081
	Case 3	1415.9543	15.9290	1262.4783	279.3751	1404.8571	35.4639
	Case 4	0.0012	1.9E-05	0.0008	0.0002	0.0008	0.0001
	Case 5	131.2993	1.2541	108.8925	32.2528	124.7196	2.7010
	Case 6	13.7659	0.3423	10.3615	2.7929	13.6254	0.1453
	Case 7	14022.7038	209.2153	13180.9795	1491.0045	13683.3289	439.0254
	Case 8	29253.4445	2944.9541	25983.6193	7547.0732	23893.4368	5345.2839

TABLE XVII
THE AVERAGE ELAPSED TIME

Algorithms	the average elapsed time (second)									
	Case 1	Case 2	Case 3	Case 4	Case 5	Case 6	Case 7	Case 8	Case 9	Case 10
MHFPA	194.585	190.379	189.642	193.938	230.887	199.520	495.278	489.382	1441.446	1506.057
NSGA-II	216.852	219.469	193.980	206.600	241.549	196.369	503.592	478.379	1496.931	1657.499
MOPSO	224.766	229.502	185.914	237.663	248.277	202.895	518.947	499.232	-	-

problems. This paper takes eight optimization experiments performed on IEEE30 and IEEE57 bus systems as examples to study the optimization performance of MHFPA, MOPSO and NSGA-II algorithms more comprehensively.

1) SP

SP index represents the standard deviation of adjacent solutions in non-dominant solutions. A detailed introduction of SP is given in Reference [11]. The calculation formula of SP is as follows:

$$SP=\sqrt{\frac{1}{n-1}\sum_{i=1}^{n}(D_{mean}-d_i)^2} \tag{36}$$

$$d_i=\min_{j=1,2,\dots n}\left(\sum_{k=1}^{M}\left|f_k^i-f_k^j\right|\right) \tag{37}$$

$$D_{mean}=\frac{1}{n}\sum_{i}^{n}d_i \tag{38}$$

where D_{mean} is the average value of all d_i. The SP index reflects the distribution of POS set on the simulation graph. In general, the smaller the value of this index is, the more evenly distributed the solutions in the POS are. If SP=0, it means that there are equal intervals among the solutions in the Pareto optimal front.

2) HV

HV measures the coverage of Pareto front in the feasible region space. The larger the value of this index is, the more widely the solution set of the Pareto front is distributed in the feasible region. The detailed introduction of HV is given in Reference [19]. The definition of HV index is shown in Equation (39).

$$HV=volume\left(\bigcup_{i=1}^{n}v_i\right) \tag{39}$$

where v_i represents the area or volume formed by each individual i in the solution set and the selected reference point.

3) Statistical Analysis

All the above analyses are the best simulation results of 20 independent running experiments for MHFPA, MOPSO and NSGA-II algorithms. In this section, we will calculate the SP and HV performance indicators of the 20 running results of the three algorithms in case 1-case 8, and use box plots to visually express the statistical data of the SP and HV. TABLE XVI shows the detailed evaluation results of the SP and HV indicators. In the box plot, there is a line in the middle of the box, which represents the median of the data. Its height reflects the volatility of the data, and the top and bottom represent the maximum and minimum values of this set of data, respectively. Sometimes there are dots on the outside of the box that can be interpreted as outliers.

Fig. 17 shows the box plots of the SP indicators of 8 cases. It can be seen from the figure, the fluctuation of SP index data of MHFPA is the least, and its average values are the lowest in most cases. This shows that the proposed algorithm is more stable and the distribution of the solution set is more uniform than the other two algorithms. In Case2, Case3 and Case5, although the MHFPA algorithm fails to obtain the minimum SP mean value, MHFPA has fewer outliers than other methods, and the Pareto front and BTS obtained by this algorithm in the simulation cases are superior to the two comparison algorithms.

Fig. 18 shows the box plots of the HV indicators of 8 cases. It can be seen from the figure that MHFPA algorithm obtained the minimum HV standard deviation value, indicating that the diversity difference of Pareto front obtained by this algorithm in 20 independent experiments is smaller than other algorithms. In addition, the HV index data of this algorithm has fewer outliers, and its average value is larger than that of other methods, which proves that the PF solution set obtained by this algorithm has better diversity.

TABLE XVIII
THE BEST SOLUTIONS OF CASE 10

control variables	MHFPA	NSGA-II	control variables	MHFPA	NSGA-II
P_{Ge_4} (MW)	5.1945	6.1521	V_{Ge_26}	1.0309	1.0013
P_{Ge_6}	8.0653	12.2689	V_{Ge_27}	1.0473	1.0410
P_{Ge_8}	5.0000	11.8057	V_{Ge_31}	1.0471	1.0236
P_{Ge_10}	282.1645	189.4110	V_{Ge_32}	1.0092	0.9712
P_{Ge_12}	286.4341	181.1385	V_{Ge_34}	1.0024	0.9897
P_{Ge_15}	10.0725	20.6620	V_{Ge_36}	1.0418	1.0195
P_{Ge_18}	31.0743	51.0332	V_{Ge_40}	1.0303	0.9317
P_{Ge_19}	5.8439	7.6006	V_{Ge_42}	0.9793	1.0135
P_{Ge_24}	5.7036	6.3380	V_{Ge_46}	1.0411	1.0011
P_{Ge_25}	100.8793	100.1967	V_{Ge_49}	1.0130	1.0256
P_{Ge_26}	100.0000	154.5302	V_{Ge_54}	1.0080	1.0146
P_{Ge_27}	8.0000	13.2450	V_{Ge_55}	1.0153	1.0286
P_{Ge_31}	8.0555	9.8663	V_{Ge_56}	1.0197	1.0057
P_{Ge_32}	52.4531	25.3440	V_{Ge_59}	1.0355	0.9942
P_{Ge_34}	8.0000	15.7428	V_{Ge_61}	1.0491	1.0044
P_{Ge_36}	27.2354	32.3629	V_{Ge_62}	1.0398	1.0423
P_{Ge_40}	9.9334	13.9711	V_{Ge_65}	1.0402	0.9840
P_{Ge_42}	8.3585	17.6326	V_{Ge_66}	1.0547	1.0305
P_{Ge_46}	61.4959	35.4225	V_{Ge_69}	1.0070	0.9844
P_{Ge_49}	248.1737	249.9834	V_{Ge_70}	0.9901	1.0293
P_{Ge_54}	51.1580	151.2727	V_{Ge_72}	1.0367	0.9938
P_{Ge_55}	33.2710	50.2628	V_{Ge_73}	0.9941	1.0697
P_{Ge_56}	26.1296	30.7026	V_{Ge_74}	1.0064	0.9282
P_{Ge_59}	63.0469	50.0540	V_{Ge_76}	1.0038	1.0172
P_{Ge_61}	200.0000	176.7912	V_{Ge_77}	1.0393	1.0322
P_{Ge_62}	29.5615	90.7788	V_{Ge_80}	1.0247	0.9884
P_{Ge_65}	410.5184	304.1519	V_{Ge_85}	0.9765	1.0262
P_{Ge_66}	244.6302	245.9660	V_{Ge_87}	1.0120	1.0024
P_{Ge_69}	34.4022	53.0422	V_{Ge_89}	1.0438	1.0085
P_{Ge_70}	10.1921	10.4304	V_{Ge_90}	0.9962	1.0274
P_{Ge_72}	5.3894	7.5431	V_{Ge_91}	1.0180	1.0109
P_{Ge_73}	5.0496	5.0374	V_{Ge_92}	1.0470	1.0036
P_{Ge_74}	31.5602	60.1638	V_{Ge_99}	1.0801	1.0535
P_{Ge_76}	31.3947	51.0609	V_{Ge_100}	1.0114	1.0281
P_{Ge_77}	238.4564	221.5711	V_{Ge_103}	0.9861	0.9976
P_{Ge_80}	34.9182	71.4405	V_{Ge_104}	1.0066	0.9819
P_{Ge_85}	10.0000	16.7094	V_{Ge_105}	0.9994	0.9772
P_{Ge_87}	186.6442	236.9483	V_{Ge_107}	0.9387	0.9543
P_{Ge_89}	118.5274	82.2049	V_{Ge_110}	0.9998	1.0087
P_{Ge_90}	8.0615	9.3205	V_{Ge_111}	0.9467	1.0928
P_{Ge_91}	20.0000	25.3201	V_{Ge_112}	1.0305	0.9781
P_{Ge_92}	130.9848	173.5649	V_{Ge_113}	1.0477	0.9918
P_{Ge_99}	153.4428	114.5672	V_{Ge_116}	1.0775	1.0030
P_{Ge_100}	172.2901	111.4755	T_8 (p.u.)	0.1100	0.0250
P_{Ge_103}	8.0000	10.2722	T_{32}	0.0346	0.1639
P_{Ge_104}	26.2246	25.2439	T_{36}	0.1090	0.0365
P_{Ge_105}	34.9555	25.0000	T_{51}	0.0864	0.1171
P_{Ge_107}	8.4857	8.1347	T_{93}	0.0013	0.1504
P_{Ge_110}	25.2492	32.1845	T_{95}	0.1504	0.1755
P_{Ge_111}	25.0000	40.1529	T_{102}	0.0436	0.1790
P_{Ge_112}	27.3803	49.7732	T_{107}	0.0108	0.0663
P_{Ge_113}	39.8090	48.8245	T_{127}	0.0291	0.1621
P_{Ge_116}	26.2157	32.1997	Q_{Co_34} (p.u.)	0.0053	0.1413
V_{Ge_1} (p.u.)	1.0926	1.0364	Q_{Co_44}	0.1064	0.0670
V_{Ge_4}	1.0868	1.0256	Q_{Co_45}	0.2682	0.1577
V_{Ge_6}	1.0882	0.9701	Q_{Co_46}	0.0470	0.1611
V_{Ge_8}	0.9790	0.9757	Q_{Co_48}	0.2373	0.0995
V_{Ge_10}	1.0564	0.9900	Q_{Co_74}	0.2703	0.1676
V_{Ge_12}	1.0090	0.9951	Q_{Co_79}	0.2277	0.2532
V_{Ge_15}	1.0243	0.9566	Q_{Co_82}	0.0000	0.2972
V_{Ge_18}	1.0112	1.0013	Q_{Co_83}	0.2184	0.2250
V_{Ge_19}	0.9354	1.0153	Q_{Co_105}	0.1333	0.1695
V_{Ge_24}	1.0803	0.9428	Q_{Co_107}	0.2528	0.0882
V_{Ge_25}	0.9176	1.0335	Q_{Co_110}	0.0136	0.0026
			J_{fcost} (\$/h)	**59455.5016**	60271.7117
			$J_{emission}$ (ton/h)	**2.2220**	2.8592

G. *Algorithm Complexity*

The algorithm complexity can be used as the evaluation index of algorithm efficiency, which is indirectly expressed by the average running time in this paper. In the face of practical engineering problems, the dispatcher definitely hopes that the algorithm can be efficient in solving the power flow optimization problem. TABLE XVII shows the average elapsed time of the three algorithms running independently 20 times in cases 1-10. It can be seen from the table that MHFPA takes less time to solve the MOOPF problem than the

NSGA-II and MOPSO algorithms, thus further verifying the efficiency of the algorithm.

V. Conclusion

This paper proposes a modified and hybrid flower pollination algorithms named MHFPA, including the mutation and crossover process in the DE algorithm, the sinusoidal nonlinear dynamic switching probability and the elite strategy of elder generation to solve the MOOPF problem. In this paper, different multi-objectives, which consider the total fuel cost, active power loss, total fuel cost with valve point, emissions and voltage deviation impacts, for OPF problem are formed. The IEEE30-, 57- and IEEE118-bus test systems with ten cases under the condition of satisfying the equality and inequality constraints are used to test the effectiveness of the proposed MHFPA. In order to obtain a well-distributed Pareto front, three multi-objective optimization strategies are introduced: SPA, NSES and BTS. Two performance indicators, HV and SP, comprehensively evaluate the performance of the proposed algorithm. Compared with the experimental results, MHFPA has more competitive advantages than MOPSO and NSGA-II algorithms in solving MOOPF problems. Therefore, the proposed MHFPA algorithm is a good candidate to solve the MOOPF problem in the real power system.

References

[1] E. Naderi, M. Pourakbari-Kasmaei and H. Abdi, "An efficient particle swarm optimization algorithm to solve optimal power flow problem integrated with FACTS devices," *Applied Soft Computing*, vol. 80, pp. 243-262, 2019.

[2] A. Attia, R. A. El Sehiemy and H. M. Hasanien, "Optimal power flow solution in power systems using a novel Sine-Cosine algorithm," *International Journal of Electrical Power & Energy Systems*, vol. 99, pp. 331-343, 2018.

[3] S. Rahmani and N. Amjady, "Enhanced goal attainment method for solving multi-objective security-constrained optimal power flow considering dynamic thermal rating of lines," *Applied Soft Computing*, vol. 77, pp. 41-49, 2019.

[4] S. A. El-Sattar, S. Kamel, R. A. El Sehiemy, F. Jurado, J. Yu and L. Mei, et al., "Single- and multi-objective optimal power flow frameworks using Jaya optimization technique," *Neural Computing & Applications*, vol. 31, no. 12, pp. 8787-8806, 2019.

[5] G. Chen, X. Yi, Z. Zhang and H. Lei, "Solving the Multi-Objective Optimal Power Flow Problem Using the Multi-Objective Firefly Algorithm with a Constraints-Prior Pareto-Domination Approach," *Energies*, vol. 11, no. 12, pp. 3438, 2018.

[6] G. Chen, J. Qian, Z. Zhang and Z. Sun, "Multi-objective Improved Bat Algorithm for optimizing fuel cost, emission and active power loss in power system," *IAENG International Journal of Computer Science*, vol. 46, no. 1, pp. 118-133, 2019.

[7] G. Chen, Y. Han, Z. Zhang, X. Zeng and S. Li, "Research on Multi-objective Active Power Optimization Simulation of Novel Improved Water Cycle Algorithm," *IAENG International Journal of Applied Mathematics*, vol. 51, no. 1, pp. 250-263, 2021.

[8] G. Chen, J. Qian, Z. Zhang and Z. Sun, "Applications of Novel Hybrid Bat Algorithm With Constrained Pareto Fuzzy Dominant Rule on Multi-Objective Optimal Power Flow Problems," *IEEE Access*, vol. 7, pp. 52060-52084, 2019.

[9] N. Daryani, M. T. Hagh and S. Teimourzadeh, "Adaptive group search optimization algorithm for multi-objective optimal power flow problem," *Applied Soft Computing*, vol. 38, pp. 1012-1024, 2016.

[10] R. V. Rao, D. P. Rai and J. Balic, "Multi-objective optimization of machining and micro-machining processes using non-dominated sorting teaching-learning-based optimization algorithm," *Journal of Intelligent Manufacturing*, vol. 29, no. 8, pp. 1715-1737, 2018.

[11] T. Ding, C. Li, F. Li, T. Chen and R. Liu, "A bi-objective DC-optimal power flow model using linear relaxation-based second order cone programming and its Pareto Frontier," *International Journal of Electrical Power & Energy Systems*, vol. 88, pp. 13-20, 2017.

[12] R. Storn andK. Price, "Differential evolution - A simple and efficient heuristic for global optimization over continuous spaces," *Journal of Global Optimization*, vol. 11, no. 4, pp. 341-359, 1997.

[13] S. Mirjalili, "Moth-flame optimization algorithm: A novel nature-inspired heuristic paradigm," *Knowledge-Based Systems*, vol. 89, pp. 228-249, 2015.

[14] K. Deb, A. Pratap, S. Agarwal and T. Meyarivan, "A fast and elitist multiobjective genetic algorithm: NSGA-II," *IEEE Transactions on Evolutionary Computation*, vol. 6, no. 2, pp. 182-197, 2002.

[15] M. Clerc and J. Kennedy, "The particle swarm - Explosion, stability, and convergence in a multidimensional complex space," *IEEE Transactions on Evolutionary Computation*, vol. 6, no. 1, pp. 58-73, 2002.

[16] Y. Yuan, Y. Yuan, X. Wu and X. Wu, et al., "Application of improved bat algorithm in optimal power flow problem," *Applied intelligence (Dordrecht, Netherlands)*, vol. 48, no. 8, pp. 2304-2314, 2018.

[17] E. Naderi, M. Pourakbari-Kasmaei, F. V. Cerna and M. Lehtonen, "A novel hybrid self-adaptive heuristic algorithm to handle single- and multi-objective optimal power flow problems," *International Journal of Electrical Power & Energy Systems*, vol. 125, article. 106492 (1-17), 2021.

[18] W. Warid, H. Hizam, N. Mariun and N. I. Abdul Wahab, "A novel quasi-oppositional modified Jaya algorithm for multi-objective optimal power flow solution," *Applied Soft Computing*, vol. 65, pp. 360-373, 2018.

[19] J. Qian, P. Wang, C. Pu and G. Chen, "Joint application of multi-object beetle antennae search algorithm and BAS-BP fuel cost forecast network on optimal active power dispatch problems," *Knowledge-Based Systems*, vol. 226, article. 107149 (1-21), 2021.

[20] M. Ding, H. Chen, N. Lin, S. Jing, F. Liu and X. Liang, et al., "Dynamic population artificial bee colony algorithm for multi-objective optimal power flow," *Saudi Journal of Biological Sciences*, vol. 24, no. 3, pp. 703-710, 2017.

[21] M. A. Taher, S. Kamel, F. Jurado and M. Ebeed, "An improved moth-flame optimization algorithm for solving optimal power flow problem," *International Transactions on Electrical Energy Systems*, vol. 29, no. 3, article. e2743 (1-28), 2019.

[22] G. Chen, J. Qian, Z. Zhang and S. Li, "Application of modified pigeon-inspired optimization algorithm and constraint -objective sorting rule on multi-objective optimal power flow problem," *Applied Soft Computing*, vol. 92, article. 106321 (1-19), 2020.

[23] G. Chen, X. Yi, Z. Zhang and H. Wang, "Applications of multi-objective dimension-based firefly algorithm to optimize the power losses, emission, and cost in power systems," *Applied Soft Computing*, vol. 68, pp. 322-342, 2018.

[24] G. Chen, J. Qian, Z. Zhang and Z. Sun, "Multi-Objective Optimal Power Flow Based on Hybrid Firefly-Bat Algorithm and Constraints-Prior Object-Fuzzy Sorting Strategy," *IEEE Access*, vol. 7, pp. 139726-139745, 2019.

[25] X. Yang, M. Karamanoglu and X. He, "Flower pollination algorithm: A novel approach for multiobjective optimization," *Engineering Optimization*, vol. 46, no. 9, pp. 1222-1237, 2014.

[26] M. Abdel-Basset, M. Abdel-Basset, L. A. Shawky and L. A. Shawky, "Flower pollination algorithm: a comprehensive review," *Artificial Intelligence Review*, vol. 52, no. 4, pp. 2533-2557, 2019.

[27] A. Fouad and X. Gao, "A novel modified flower pollination algorithm for global optimization," *Neural Computing & Applications*, vol. 31, no. 8, pp. 3875-3908, 2019.

[28] P. P. Biswas, P. N. Suganthan, R. Mallipeddi and G. A. J. Amaratunga, "Multi-objective optimal power flow solutions using a constraint handling technique of evolutionary algorithms," *Soft computing (Berlin, Germany)*, vol. 24, no. 4, pp. 2999-3023, 2020.

[29] S. R. Salkuti, "Optimal power flow using multi-objective glowworm swarm optimization algorithm in a wind energy integrated power system," *International Journal of Green Energy*, vol. 16, no. 15, pp. 1547-1561, 2019.

[30] B. Ji, X. Yuan and Y. Yuan, "Modified NSGA-II for Solving Continuous Berth Allocation Problem: Using Multiobjective Constraint-Handling Strategy," *IEEE Transactions on Cybernetics*, vol. 47, no. 9, pp. 2885-2895, 2017.

[31] A. A. Mohamed, Y. S. Mohamed, A. A. M. El-Gaafary and A. M. Hemeida, "Optimal power flow using moth swarm algorithm," *Electric Power Systems Research*, vol. 142, pp. 190-206, 2017.

[32] S. Rahmani and N. Amjady, "Improved normalised normal constraint method to solve multi-objective optimal power flow problem," *IET generation, transmission & distribution*, vol. 12, no. 4, pp. 859-872, 2018.

[33] H. Pulluri, R. Naresh and V. Sharma, "An enhanced self-adaptive differential evolution based solution methodology for multiobjective optimal power flow," *Applied Soft Computing*, vol. 54, pp. 229-245, 2017.
[34] A. Sundaram, "Multiobjective multi-verse optimization algorithm to solve combined economic, heat and power emission dispatch problems," *Applied Soft Computing*, vol. 91, article. 106195 (1-24), 2020.
[35] W. Zhang, Z. Qu, K. Zhang, W. Mao, Y. Ma and X. Fan, "A combined model based on CEEMDAN and modified flower pollination algorithm for wind speed forecasting," *Energy Conversion and Management*, vol. 136, pp. 439-451, 2017.
[36] V. Porkodi, A. R. Singh, A. R. W. Sait, K. Shankar, E. Yang and C. Seo, et al, "Resource Provisioning for Cyber–Physical–Social System in Cloud-Fog-Edge Computing Using Optimal Flower Pollination Algorithm," *IEEE Access*, vol. 8, pp. 105311-105319, 2020.
[37] X. Liang, W. Liang and J. Xiong, "Intelligent diagnosis of natural gas pipeline defects using improved flower pollination algorithm and artificial neural network," *Journal of Cleaner Production*, vol. 264, article. 121655 (1-16), 2020.
[38] R. Salgotra and U. Singh, "Application of mutation operators to flower pollination algorithm," *Expert Systems with Applications*, vol. 79, pp. 112-129, 2017.
[39] W. Deng, J. Xu, Y. Song and H. Zhao, "Differential evolution algorithm with wavelet basis function and optimal mutation strategy for complex optimization problem," *Applied Soft Computing*, vol. 100, article. 106724 (1-16), 2021.
[40] T. Niknam, M. R. Narimani, M. Jabbari and A. R. Malekpour, "A modified shuffle frog leaping algorithm for multi-objective optimal power flow," *Energy*, vol. 36, no. 11, pp. 6420-6432, 2011.